A novel class of multitarget anti-Alzheimer benzohomoadamantane–chlorotacrine hybrids modulating cholinesterases and glutamate NMDA receptors

A novel class of multitarget anti-Alzheimer benzohomoadamantane–chlorotacrine hybrids modulating cholinesterases and glutamate NMDA receptors

F. Javier Pérez-Areales[a], Andreea L. Turcu[a], Marta Barniol-Xicota[a], Caterina Pont[a], Deborah Pivetta[a], Alba Espargaró[b], Manuela Bartolini[c], Angela De Simone[d], Vincenza Andrisano[d], Belén Pérez[e], Raimon Sabate[b], Francesc X. Sureda[f], Santiago Vázquez[a,*], Diego Muñoz-Torrero[a,*]

[a] *Laboratory of Pharmaceutical Chemistry (CSIC Associated Unit), Faculty of Pharmacy and Food Sciences, and Institute of Biomedicine (IBUB), University of Barcelona, Av. Joan XXIII 27-31, E-08028 Barcelona, Spain*

[b] *Department of Pharmacy and Pharmaceutical Technology and Physical-Chemistry, Faculty of Pharmacy and Food Sciences, and Institute of Nanoscience and Nanotechnology (IN2UB), University of Barcelona, Av. Joan XXIII 27-31, E-08028 Barcelona, Spain*

[c] *Department of Pharmacy and Biotechnology, Alma Mater Studiorum University of Bologna, Via Belmeloro 6, I-40126 Bologna, Italy*

[d] *Department for Life Quality Studies, Alma Mater Studiorum University of Bologna, Corso d'Augusto 237, I-47921 Rimini, Italy*

[e] *Department of Pharmacology, Therapeutics, and Toxicology, Autonomous University of Barcelona, E-08193 Bellaterra, Spain*

[f] *Pharmacology Unit, Faculty of Medicine and Health Sciences, Universitat Rovira i Virgili, c/St. Llorenç 21, E-43201 Reus, Spain*

* Corresponding authors. Tel.: +34 934024533; *E-mail addresses: svazquez@ub.edu (S. Vázquez); dmunoztorrero@ub.edu (D. Muñoz-Torrero).*

ABSTRACT

The development of multitarget compounds against multifactorial diseases, such as Alzheimer's disease, is an area of very intensive research, due to the expected superior therapeutic efficacy that should arise from the simultaneous modulation of several key targets of the complex pathological network. Here we describe the synthesis and multitarget biological profiling of a new class of compounds designed by molecular hybridization of an NMDA receptor antagonist fluorobenzohomoadamantanamine with the potent acetylcholinesterase (AChE) inhibitor 6-chlorotacrine, using two different linker lengths and linkage positions, to preserve or not the memantine-like polycyclic unsubstituted primary amine. The best hybrids exhibit greater potencies than parent compounds against AChE (IC_{50} 0.33 nM in the best case, 44-fold increased potency over 6-chlorotacrine), butyrylcholinesterase (IC_{50} 21 nM in the best case, 24-fold increased potency over 6-chlorotacrine), and NMDA receptors (IC_{50} 0.89 μM in the best case, 2-fold increased potency over the parent benzohomoadamantanamine and memantine), which suggests an additive effect of both pharmacophoric moieties in the interaction with the primary targets. Moreover, most of these compounds have been predicted to be brain permeable. This set of biological properties makes them promising leads for further anti-Alzheimer drug development.

Keywords: Multitarget compounds
Multi-target-directed ligands
Acetylcholinesterase inhibitors
Butyrylcholinesterase inhibitors
NMDA antagonists
Brain permeability

1. Introduction

Alzheimer's disease (AD) is a chronic neurodegenerative disorder that causes cognitive impairment and inexorably leads to dementia and death. With age being the main risk factor, the societal burden of AD in an increasingly aging population is reaching alarming proportions worldwide. The most worrisome predictions about AD prevalence, mortality, and associated economic costs are being continuously exceeded [1], thereby putting health systems and national economies at unmanageable risk if current drug discovery efforts do not result in efficacious treatments.

Only four drugs are currently used for AD treatment, namely the acetylcholinesterase (AChE) inhibitors donepezil, galantamine, and rivastigmine, and the glutamate NMDA receptor antagonist memantine. These drugs address the marked impairment in neurotransmitter systems, prominently the cholinergic and the glutamatergic system that occur in AD patients as a consequence of synaptic dysfunction and neuronal death, which is one of the main histopathological hallmarks of AD. Other two common features are senile plaques and neurofibrillary tangles, which result from overproduction and aggregation of β-amyloid peptide (Aβ) and hyperphosphorylation and aggregation of tau protein, respectively. Despite some evidence of disease-modifying effects by the currently approved anti-Alzheimer drugs [2-7], they are regarded and used as symptomatic drugs. Since the launching of these drugs, research efforts have pursued the development of alternative neurotransmitter-based symptomatic therapies and, mainly, new drugs that act specifically on a given biological target or event with a prominent pathogenic role, in most cases related to Aβ and tau biology. Unfortunately, the enormous amounts of research efforts and resources that have been invested in the past three decades have not been corresponded by the discovery of novel drugs that have proven capable of halting or even just slowing down the neurodegenerative processes occurring in this fatal disease. Indeed, AD is one of the therapeutic areas with the highest attrition rates in clinical trials [8,9]. Very disappointingly, no drug candidate has successfully passed phase III clinical trials for AD since the launching of memantine, almost two decades ago.

The repetitive failures of very promising target-specific drugs in clinical trials is leading to a growing awareness of the complex multifactorial nature of AD, which could result from the dysregulation of multiple separate but integrated signaling pathways. A scenario of a complex pathogenic network would account for the lack of efficacy of drugs that address a particular signaling pathway by modulation of a single biological

target, and warrants the development of alternative therapeutic approaches based on the simultaneous modulation of several crucial biological targets, which should result in additive or synergistic effects [10,11]. Multitarget treatments may involve the use of several specific drugs (drug cocktails or fixed-dose combinations) or a single drug with the ability to hit several biological targets (multitarget drugs). Even though the design and development of multitarget drugs can be very challenging [12], it has some clear advantages over multiple-medication therapies, such as simpler dose regimens and improved patient compliance, simpler pharmacokinetics and lack of drug–drug interactions, and simpler clinical development, among others [13,14]. In fact, both strategies are being currently used in AD treatment or pursued in AD drug discovery. On the one hand, the combination of the AChE inhibitor donepezil with the glutamate NMDA antagonist memantine has proven to lead to additive or synergistic effects in mouse models and AD patients [15–17], and a fixed-dose combination of both drugs (Namzaric®) is now being used as the standard of care to treat dementia associated with moderate to severe stages of the disease [18,19]. On the other hand, AD is one of the therapeutic areas where the development of multitarget drugs has been more intensively pursued in the past decade [20–22]. Most of these compounds are hybrids that combine distinct pharmacophoric moieties to confer multiple activities [for recent examples see 23–37]. A crucial point in the design of multitarget anti-Alzheimer compounds is the selection of the biological targets to hit, and, hence, of the pharmacophores to be used. Many different combinations of targets have been considered, with most of them including AChE. Particularly, the mechanism of action of the currently marketed anti-Alzheimer drugs and the fact that the combination of both mechanisms in the fixed-dose combination of an AChE inhibitor (donepezil) and a glutamate NMDA receptor antagonist (memantine) results in improved clinical efficacy have provided a valuable clue for the design of hybrid compounds that combine pharmacophoric moieties to impart those activities [38–40]. Some of these compounds feature a moiety of a well-known AChE inhibitor, such as galantamine or 7-methoxytacrine [41], linked through an oligomethylene tether to a memantine or the closely related amantadine unit (compounds **3**-**5**, Figure 1) [42–45]. These compounds exhibit nanomolar to submicromolar AChE inhibitory activities and low micromolar affinities towards glutamate NMDA receptors, slightly lower than that of memantine. Very interestingly, one of them, ARN14140, gave cognition enhancing effects and balanced the levels of biomarkers of neurodegeneration, synaptic plasticity, and apoptosis in a non-transgenic

mouse model of AD [43], thereby highlighting the therapeutic potential of the combination of AChE inhibition and NMDA receptor antagonism in a single multitarget molecule.

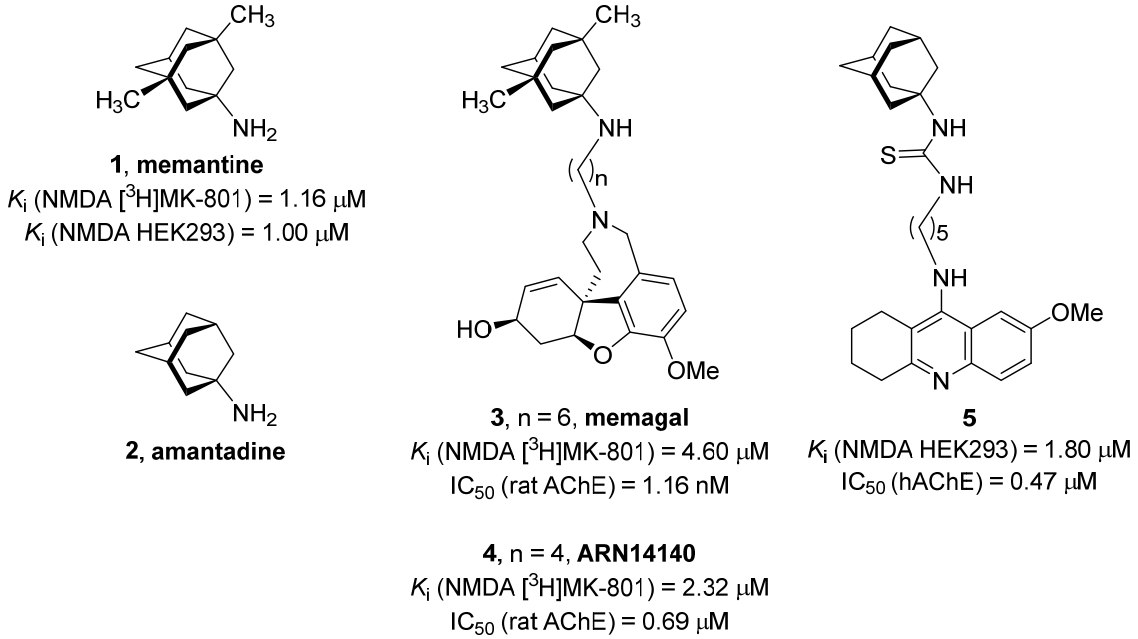

Fig. 1. Structures of memantine, amantadine, and derivatives **3**-**5** with dual glutamate NMDA receptor affinity and AChE inhibitory activity.

During the past decade we have been exploring the glutamate NMDA receptor antagonistic activity of novel polycyclic amines featuring oxaadamantane [46], noradamantane and bisnoradamantane [47], benzohomooxaadamantane [48], and benzohomoadamantane [49,50] scaffolds, as bioisosteric, ring-contracted or ring-expanded analogs of memantine. Among these compounds, the fluorobenzohomoadamantanamine **6** (Figure 2) and its non-fluorinated analog turned out to be the most potent NMDA receptor antagonists, with potencies very close to that of memantine in a functional assay in rat cultured cerebellar granule neurons (CGN) [50].

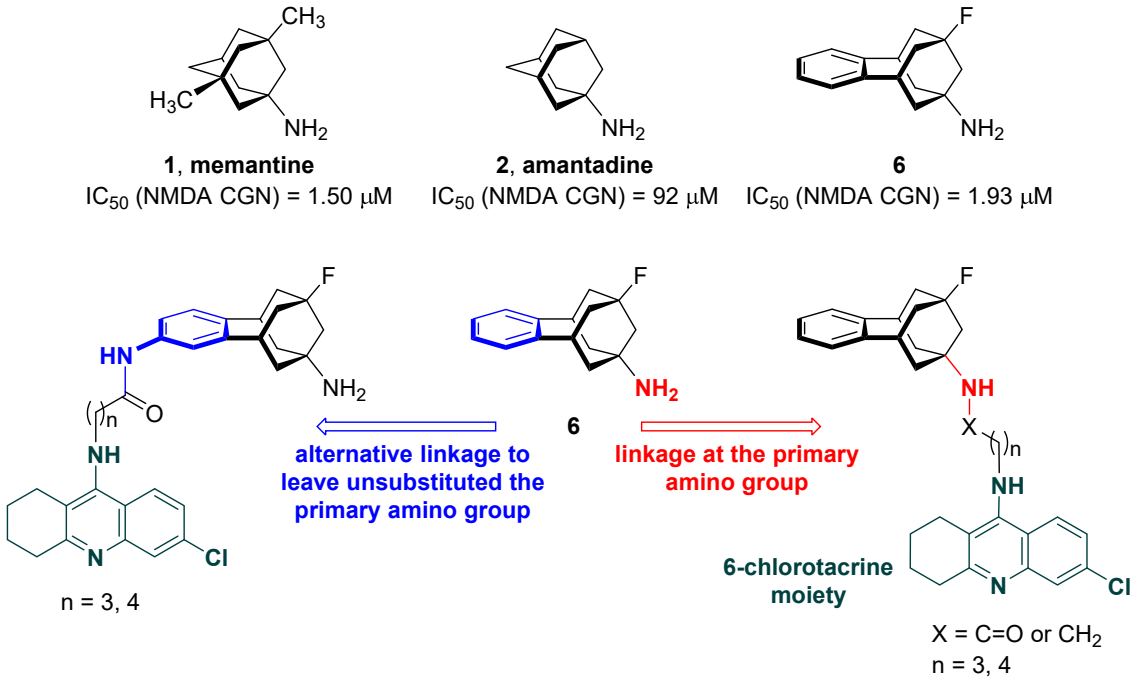

Fig. 2. Structure of the benzohomoadamantanamine **6** and design of the novel hybrids derived from **6** and the AChE inhibitor 6-chlorotacrine.

The proven therapeutic potential of the combination of glutamate NMDA receptor antagonism with AChE inhibition, the interesting NMDA antagonistic activity of the benzohomoadamantanamine **6**, and our own experience in the development of multitarget anti-Alzheimer compounds containing AChE inhibitor pharmacophores [51–54] prompted us to undertake the design of a novel class of multitarget hybrid compounds featuring the aminopolycyclic scaffold of **6** and a unit of the potent AChE inhibitor 6-chlorotacrine [55] (Figure 2). In all memantine- or amantadine-based multitarget hybrids previously reported, the aminopolycyclic moiety is linked to the AChE inhibitor moiety through the amino group. It has been reported that alkylation (monomethylation) of the amino group of memantine leads to a twofold decrease of affinity and antagonistic activity towards NMDA receptors, whereas dialkylation has a much more dramatic effect (3-fold reduced affinity and 12-fold reduced NMDA antagonistic activity) [56]. This trend was also observed in some of the polycyclic amines we had developed as NMDA receptor antagonists [47,49,50], but not in all of them [46,48]. To further shed light on this, we envisaged the synthesis of two short series of benzohomoadamantane–chlorotacrine hybrids, where the attachment point of the aminopolycyclic moiety to the rest of the molecule was either the bridgehead aliphatic primary amino group or a second amino group placed at the benzene ring,

thereby leaving unsubstituted the "memantine-like" aliphatic amino group (Figure 2). A linker length similar to that used in the previously reported memantine- or amantadine-based multitarget compounds was envisaged for the novel benzohomoadamantane–chlorotacrine hybrids.

Here we report the synthesis of this novel class of benzohomoadamantane–chlorotacrine hybrids and their *in vitro* biological profiling, including the determination of their inhibitory activity against both human cholinesterases (human AChE (hAChE) and human butyrylcholinesterase (hBChE)), glutamate NMDA receptor antagonistic activity, and brain permeability. Because other families of 6-chlorotacrine-related hybrids developed in our group have shown activity against the enzyme BACE-1 (β-secretase) and Aβ42 and tau aggregation [51–54], the novel benzohomoadamantane–chlorotacrine hybrids were also evaluated against these other targets of interest in AD treatment.

2. Results and discussion

2.1. Synthesis of the novel benzohomoadamantane–chlorotacrine hybrids

The synthesis of the target hybrids **13a** and **13b**, in which the benzohomoadamantanamine moiety was linked throught its primary amino group to the chlorotacrine unit, was carried out by the alternative sequences depicted in Scheme 1, using 6-chlorotacrine, **7** [55], or the dichloroacridine derivative **8** [57] as the starting materials. We initially envisaged a four-step route that involved alkylation of 6-chlorotacrine with the appropriate ω-bromoalkanenitrile, followed by hydrolysis of the cyano group, amide coupling of the resulting carboxylic acid with the benzohomoadamantanamine **6**, and final reduction of the amide to the secondary amine. Reaction of 6-chlorotacrine, **7**, with 5-bromovaleronitrile, in the presence of KOH in dry DMSO led in moderate yield (64%) to the new nitrile **11b**, after silica gel column chromatography purification. However, different attempts to alkylate **7** with 4-bromobutyronitrile failed to afford the shorter homologue **11a**. The new nitrile **11a** was alternatively obtained, in 92% overall yield, by amination of the dichloroacridine derivative **8** with 3-amino-1-propanol at 135 ºC, followed by mesylation of the resulting alcohol **9a** [58], and reaction of mesylate **10a** [58] with NaCN in dry DMF (Scheme 1). Alkaline hydrolysis of nitriles **11a** and **11b**, followed by acidification with an Et_2O solution of HCl afforded the corresponding carboxylic acids, in the form of quinoline hydrochloride salts, which were directly coupled with amine **6** using EDC and HOBt, to

yield amides **12a** and **12b** in moderate yields (40% and 75% overall), after silica gel column chromatography purification. Reduction of amides **12a** and **12b** to the corresponding secondary amines turned out to be a difficult task. Different attempts of reduction with $LiAlH_4$, $LiBH_4$, or sodium bis(2-methoxyethoxy)aluminium hydride (Red-Al®) were fruitless. Finally, borane reduction of amides **12a** and **12b** did afford the target amines **13a** and **13b**, albeit in low yield (24% and 10%, respectively). Alternatively, amine **13b** was obtained by alkylation of amine **6** with mesylate **10b**, which was prepared by amination of chloroquinoline **8** with 5-amino-1-pentanol at 135 ºC, followed by mesylation of the resulting alcohol **9b**. Under these conditions, **13b** was obtained in higher yield (27%) but it was accompanied with some byproducts arising from degradation of the mesylate.

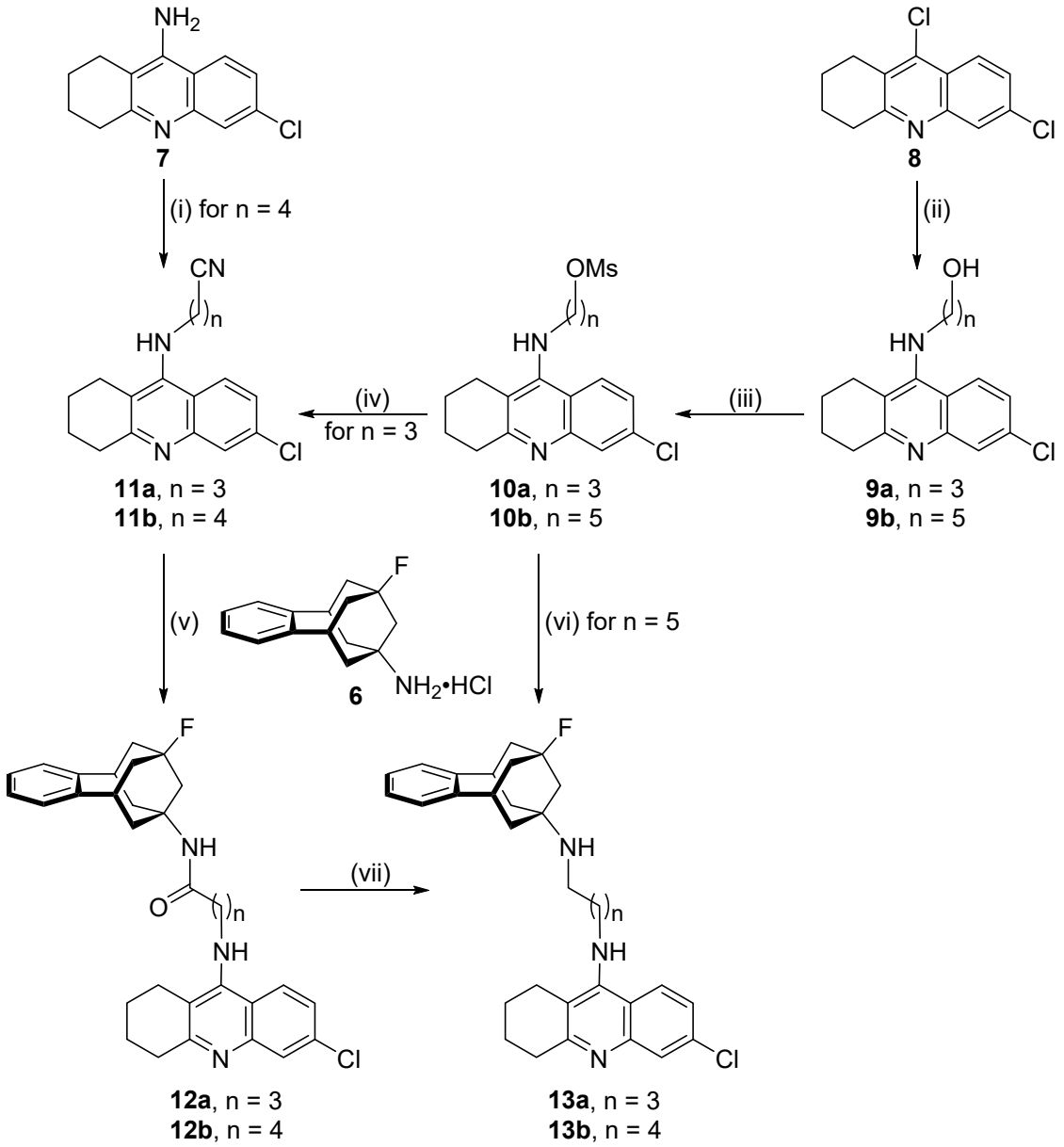

Scheme 1. Reagents and conditions: (i) **7**, KOH, DMSO, rt, 2 h; then, 5-bromovaleronitrile, rt, overnight, **11b** (64%); (ii) 3-amino-1-propanol or 5-amino-1-pentanol, 135 ºC, 1 day, **9a** (94%), **9b** (40%); (iii) MsCl, Et_3N, CH_2Cl_2, –10 ºC, 30 min, **10a** (quantitative), **10b** (quantitative); (iv) NaCN, DMF, 100 ºC, 1 h, **11a** (98%); (v) 1) 40% methanolic KOH, MeOH, reflux, 3 h; then, water, reflux, overnight; HCl / Et_2O; 2) crude carboxylic acid (quinoline hydrochloride salt), EDC·HCl, HOBt, Et_3N, EtOAc / DMF, rt, 15 min; then, **6**, EtOAc / DMF, rt, 2 days, **12a** (40% overall yield from **11a**), **12b** (75% overall yield from **11b**); (vi) **6**, K_2CO_3, DMF, 80 ºC, 2 days, **13b** (27%); (vii) BH_3·THF, THF, 0 ºC; then, rt, overnight, **13a** (24%), **13b** (10%).

The synthesis of the second set of benzohomoadamantane–chlorotacrine hybrids, **18a** and **18b**, where the chlorotacrine unit and tether chain were attached to the benzene ring of the aminopolycyclic moiety, was carried out using benzohomoadamantanamine **14**, previously prepared in our group [59], and nitriles **11a** and **11b** as the key building blocks (Scheme 2). Amine **14** was *N*-Boc-protected and then subjected to hydrogenation at atmospheric pressure and room temperature, in the presence of PtO_2 as catalyst, to afford the aniline **16** in good yield. Amide coupling of **16** with the carboxylic acids derived from hydrolysis of nitriles **11a** and **11b** led to the *N*-Boc-protected hybrids **17a** and **17b**, which, upon treatment with 4N HCl / dioxane, were converted into the target hybrids **18a** and **18b** in moderate yield (49% and 37% overall yield from **11a** and **11b**, respectively).

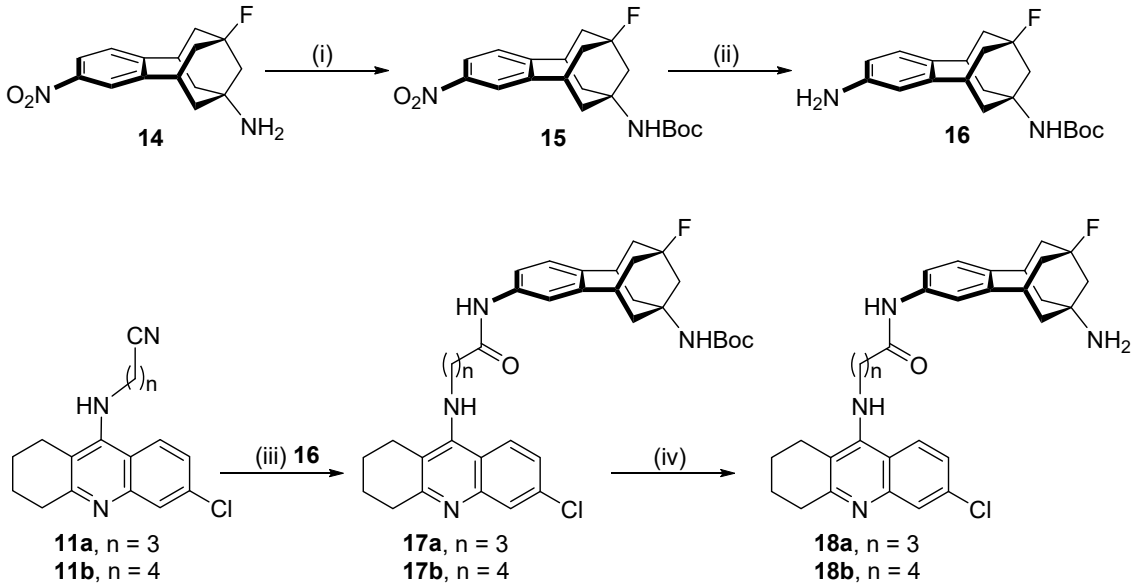

Scheme 2. Reagents and conditions: (i) 2N NaOH, di-*tert*-butyl dicarbonate, rt, 16 h, 87%; (ii) H_2, PtO_2, EtOH, 1 atm, rt, 4 h, 92%; (iii) 1) 40% methanolic KOH, MeOH, reflux, 3 h; then, water, reflux, overnight; HCl / Et_2O; 2) crude carboxylic acid (quinoline hydrochloride salt), EDC·HCl, HOBt, Et_3N, EtOAc / DMF, rt, 15 min; then, **16**, EtOAc / DMF, rt, 1 day; (iv) 4N HCl / dioxane, rt, 18 h, **18a** (49% overall yield from **11a**), **18b** (37% overall yield from **11b**).

All the benzohomoadamantane–chlorotacrine hybrids were converted into the corresponding hydrochloride or dihydrochloride salts by treatment with HCl / MeOH, prior to their chemical characterization and biological profiling.

2.2. Acetylcholinesterase and butyrylcholinesterase inhibition by the novel benzohomoadamantane–chlorotacrine hybrids

Apart from AChE, the enzyme BChE is in part responsible for the hydrolysis of the neurotransmitter acetylcholine (ACh) in the central nervous system (CNS), thereby contributing to the cholinergic deficit characteristic of AD patients. This is especially true in advanced stages of the disease, in which the levels of AChE are markedly decreased, whereas the levels of BChE remain the same or even increase, thereby acquiring a prominent role in ACh breakdown [60]. Thus, BChE inhibition or even more interestingly, dual AChE and BChE inhibition are commonly pursued in the search for novel anti-Alzheimer drug candidates. In this light, the effect of the novel benzohomoadamantane–chlorotacrine hybrids **12a**,**b**, **13a**,**b**, and **18a**,**b** on human recombinant AChE (hAChE) and human serum BChE (hBChE) was determined by the

method of Ellman *et al.* [61]. 6-Chlorotacrine, **7**, was also evaluated under the same assay conditions as a reference compound for cholinesterases inhibition (Table 1).

Table 1

Inhibitory activities against AChE and BChE, NMDA antagonistic activity, Aβ42 and tau anti-aggregating activity, and blood–brain barrier (BBB) predicted permeabilities of the benzohomoadamantane–chlorotacrine hybrids and reference compounds.

Compd	hAChE IC_{50} (nM)[a]	hBChE IC_{50} (μM)[a]	NMDA IC_{50} (μM)[b]	Aβ42 aggregation in *E. coli* (% inhib. at 10 μM)[c]	Tau protein aggregation in *E. coli* (% inhib. at 10 μM)[c]	*Pe* (10^{-6} cm s^{-1})[d] (Prediction)
12a	1.4 ± 0.1	2.3 ± 0.1	7.0 ± 2.8	< 5	10.2 ± 2.4	9.8 ± 0.9 (CNS+)
12b	1.3 ± 0.1	2.4 ± 0.2	8.3 ± 3.3	9.0 ± 1.2	12.6 ± 2.7	9.0 ± 0.5 (CNS+)
13a	2.0 ± 0.1	1.1 ± 0.1	3.3 ± 0.6	8.4 ± 2.2	22.0 ± 2.7	6.3 ± 0.1 (CNS+)
13b	1.4 ± 0.1	0.2 ± 0.0	0.9 ± 0.1	12.3 ± 2.6	20.7 ± 2.4	6.5 ± 0.3 (CNS+)
18a	0.3 ± 0.0	0.5 ± 0.0	1.2 ± 0.2	< 5	6.9 ± 3.9	2.7 ± 0.6 (CNS±)
18b	2.5 ± 0.5	0.02 ± 0.00	3.4 ± 1.2	< 5	22.9 ± 5.0	3.1 ± 0.7 (CNS±)
1	nd[e]	nd[e]	1.5 ± 0.1	nd[e]	nd[e]	nd[e]
6	nd[e]	nd[e]	1.9 ± 0.2	nd[e]	nd[e]	nd[e]
7	14.5 ± 0.9	0.5 ± 0.0	nd[e]	< 5	< 5	20 ± 0.4 (CNS+)

[a] IC_{50} inhibitory concentration (nM) towards human recombinant AChE and human serum BChE. IC_{50} values are expressed as mean ± standard error of the mean (SEM) of at least two experiments, each performed in triplicate.

[b] Functional data were obtained from primary cultures of rat CGN challenged with NMDA (100 μM, in the presence of 10 μM glycine), by measuring the intracellular calcium concentration. Data shown are expressed as mean ± SEM of at least three separate experiments carried out on three different batches of cultured cells.

[c] % Inhibition of Aβ42 and tau protein aggregation at 10 μM in intact *E. coli* cells. Values are expressed as mean ± SEM of four independent experiments (n = 4).

[d] Permeability values from the PAMPA-BBB assay. Values are expressed as the mean ± SD of three independent experiments (n = 3).

[e] Not determined.

All the novel hybrids turned out to be highly potent hAChE inhibitors, with IC_{50} values from subnanomolar (**18a**: 0.33 nM) to 2.5 nM (Table 1). Thus, the benzohomoadamantane–chlorotacrine hybrids are clearly more potent hAChE inhibitors (6–44-fold more potent) than the parent 6-chlorotacrine, **7**, which is indicative of an additive or synergistic effect by the benzohomoadamantane moiety and/or the linker. In the first series, with IC_{50} values in the very narrow range of 1.30–1.96 nM, neither the linker length nor the presence of an amide or an amine as the attachment functionality to the benzohomoadamantane core seems to play a differential role in hAChE inhibition. Thus, amines **13a**,**b** and amides **12a**,**b**, longer and shorter homologues **12a**-**13a** and **12b**-**13b** exhibited the same hAChE inhibitory potency. In contrast, in the second series, the shorter homologue **18a** was 8-fold more potent than the longer homologue **18b**. Indeed, **18a** is the most potent hAChE inhibitor among all the novel benzohomoadamantane–chlorotacrine hybrids, so that the presence of an unsubstituted primary amino group at the benzohomoadamantane core and/or the presence of an amido linkage at the benzene ring with that particular linker length seem the most favorable substitution pattern for hAChE inhibition.

In contrast to hAChE inhibition, a broader range of IC_{50} values for hBChE inhibition was found for the novel hybrids, i.e. from 21 nM (**18b**) to 2.36 μM (**12b**), as well as more defined structure–activity relationships. The presence of basic amino group at the benzohomoadamantane core seems to be important for hBChE inhibition, with secondary amines **13** being 2–11-fold more potent than their amido counterparts **12**, and with the primary amines **18**, with a different disposition of the linker, being still more potent (2–10-fold more potent than amines **13** and 5–100-fold more potent than amides **12**). Within the amines **13** and **18**, a longer tether chain leads to a 5–23-fold greater hBChE inhibitory activity. Thus, the most potent hBChE inhibitors were hybrids **13b** and **18b**, which, with IC_{50} values of 210 and 21 nM, respectively, are 2- and 24-fold more potent than the parent 6-chlorotacrine. This supports the idea that the presence of the benzohomoadamantanamine moiety in these hybrids contributes positively to the interaction with the enzyme BChE.

2.3. NMDA receptor antagonistic activity of the novel benzohomoadamantane–chlorotacrine hybrids

Apart from hAChE and hBChE, the NMDA receptor was the other primary biological target, which was pursued with the design of the benzohomoadamantane–chlorotacrine

hybrids. In particular, we inferred that the incorporation of the aminopolycyclic scaffold of the fluorobenzohomoadamantanamine **6**, an NMDA receptor antagonist developed in our group [50] that is equipotent to memantine, into the structure of the hybrids should confer this additional activity.

To assess the NMDA antagonistic activity of the novel hybrids, we performed a functional assay based on measuring their effects on the increase in intracellular calcium evoked by NMDA (100 μM, in the presence of 10 μM glycine) in cultured rat CGN loaded with Fura-2 [49]. Memantine, **1**, and fluorobenzohomoadamantanamine **6** were used as reference compounds for NMDA antagonism (Table 1).

As previously mentioned, in all the described memantine– or amantadine–AChE inhibitor hybrids, the aminopolycyclic moiety is linked to the AChE inhibitor pharmacophore through its amino group. It has been described that alkylation of the amino group of memantine is detrimental for NMDA affinity and antagonistic activity, with monomethylation leading to a twofold reduced affinity and antagonistic activity, and dialkylation producing a 3-fold and 12-fold reduction of NMDA affinity and antagonistic activity, respectively [56]. A similar trend was also observed in some polycyclic amines that were developed in our group as NMDA receptor antagonists [47,49,50], whereas the opposite trend was found in others [46,48]. In line with our previous reports, alkylation of the bridgehead amino group of the benzohomoadamantane core in the novel hybrids may lead to reduced (**13a** *vs* **6**, twofold reduction) or increased (**13b** *vs* **6**, twofold increase) NMDA antagonistic activity, with the linker length seeming to play a role (the longer homologue **13b** is 4-fold more potent than the shorter counterpart **13a**). Indeed, the most potent NMDA antagonist among the hybrids that are substituted at the bridgehead amino group, **13b**, is equipotent to the most potent hybrid featuring an unsubstituted bridgehead primary amino group, **18a**. Thus, it seems that this class of compounds can tolerate monoalkylation of the polycyclic amino group without losing NMDA antagonistic activity. However, acylation of this amino group seems to be clearly detrimental for NMDA antagonistic activity, with amides **12a** and **12b** being 2- and 9-fold less potent than amines **13a** and **13b**. These results are in agreement with those found in memantine–galantamine hybrids, where amido-linked hybrids displayed NMDA affinities 2–4-fold lower than those of the corresponding amines [42]. Therefore, the presence of a basic nitrogen atom at a bridgehead position of the polycyclic core seems to be favourable for NMDA antagonistic activity.

Overall, hybrids **13b** and **18a** are roughly twofold more potent NMDA antagonists than the parent benzohomoadamantanamine **6**, which may be indicative of an additive effect of the chlorotacrine moiety in the interaction of the hybrids with these receptors. Moreover, these novel hybrids are equipotent or slightly more potent (1.7-fold) than the NMDA antagonistic anti-Alzheimer drug memantine.

2.4. Evaluation of potential anti-amyloid activities of the novel benzohomoadamantane–chlorotacrine hybrids

It has been shown that memantine inhibits *in vitro* the aggregation of human recombinant Aβ42 in a concentration-dependent manner, through NMDA receptor-independent mechanisms [62]. Also, chronic treatment with memantine leads to reduced brain levels of insoluble Aβ and soluble Aβ oligomers in several animal models of AD. On the other hand, we have found that some classes of oligomethylene-linked 6-chlorotacrine-based hybrids can inhibit in a cell-based assay the aggregation of the two amyloidogenic proteins involved in AD pathogenesis, i.e. Aβ and tau [52]. Additionally, other families of hybrid compounds featuring a huprine moiety, closely related to 6-chlorotacrine, as AChE inhibitor pharmacophore, have been shown to inhibit *in vitro* BACE-1, the enzyme that catalyzes the first and rate-limiting step of Aβ production from the amyloid precursor protein (APP) [53,63,64], with IC_{50} values ranging from nanomolar to low micromolar.

In the light of these findings, the presence in the novel hybrids of a 6-chlorotacrine unit and a benzohomoadamantanamine moiety, structurally related to memantine, prompted us to screen them for their potential inhibitory activity on Aβ and tau aggregation and BACE-1.

To assess the Aβ and tau anti-aggregating activity of the hybrids, we used a cell-based assay in intact *Escherichia coli* cells that overexpress either Aβ42, the most aggregation-prone and neurotoxic form of Aβ, or tau, which upon expression form insoluble inclusion bodies that can be stained with thioflavin S [65,66]. When tested at an inhibitor concentration of 10 μM, low percentages of inhibition were found both for Aβ42 (up to 12%) and for tau (up to 23%) (Table 1), so these compounds are weak anti-aggregating compounds. We had found very similar results in other tacrine- and 6-chlorotacrine-based hybrids that feature a cycloaliphatic ring as the second pharmacophoric moiety [51], whereas much better anti-aggregating activities were found for 6-chlorotacrine- and huprine-based hybrids bearing as the second

pharmacophore a polycyclic heteroaromatic system [52,53,67]. Thus, the presence of an extended aromatic system, apart from that of 6-chlorotacrine or huprine, seems to be a favourable structural requirement in this class of hybrid compounds for a good anti-aggregating activity of Aβ42, tau, and other amyloidogenic protein involved in other major human disorders [67].

Finally, we assessed the *in vitro* inhibitory activity of the novel hybrids towards human recombinant BACE-1, to find that they are essentially inactive or very weak inhibitors, with percentages of inhibition up to 18% at 5 μM. Even though the presence of a chlorotacrine unit, which should be mostly protonated in the acidic endosomal compartments where BACE-1 localizes, should enable a favourable salt bridge interaction with the aspartate residues of the catalytic dyad, the weak inhibitory activity of these hybrids should result from unfavourable secondary interactions of the benzohomoadamantane moiety within the large binding site of BACE-1.

2.5. Brain permeation

CNS drugs must be able to efficiently enter into the brain by crossing the blood–brain barrier (BBB). Hybrid compounds resulting from the pharmacophore combination approach tend to have rather large molecular weights, which might compromise their ability to cross biological membranes, including BBB [68,69].

However, an increasing number of structurally diverse anti-Alzheimer hybrid compounds with molecular weights over 500 have shown good brain permeability in *in vivo* studies in mice [22]. As a preliminary assessment of brain permeability, the novel benzohomoadamantane–chlorotacrine hybrids were subjected to the parallel artificial membrane permeation assay-BBB (PAMPA-BBB), a well-established *in vitro* model of passive transcellular permeation [70]. In this method, the permeability (P_e) of the target compounds through a lipid extract of porcine brain is determined using a 70:30 mixture of phosphate-buffered saline (PBS)/EtOH. The assay was validated by correlating the experimental and reported P_e values of 14 known drugs (Section 4.2.5, Experimental Part). From the resulting linear correlation [P_e (exp) = 1.5758 P_e (lit) – 1.1459 (R^2 = 0.9241)] and the limits established by Di *et al.* for BBB permeation [70], a threshold of P_e (10^{-6} cm s^{-1}) > 5.2 was set for compounds with high BBB permeation (CNS+), and thresholds of P_e (10^{-6} cm s^{-1}) < 2.0 and 5.2 > P_e (10^{-6} cm s^{-1}) > 2.0 were established for low (CNS–) and uncertain (CNS±) BBB permeation, respectively. For the two hybrids that feature an unsubstituted bridgehead amino group, i.e. **18a** and **18b**, an uncertain

BBB permeation was predicted, whereas all the benzohomoadamantane–chlorotacrine hybrids of the first series, i.e. substituted at the bridgehead amino group, were predicted to be able to cross the BBB (Table 1), which anticipates their ability to enter the brain and reach their different CNS targets.

3. Conclusion

Molecular hybridization of the NMDA antagonist fluorobenzohomoadamantanamine **6** with the potent AChE inhibitor 6-chlorotacrine, **7**, using a 4- and 5-carbon-atom tether chain attached at the bridgehead amino group or at an additional amino group on the benzene ring of the benzohomoadamantane core, has led to a new class of multitarget compounds that share the activities of the parent compounds on their primary targets. The effect of the different linkage position is apparent in hBChE inhibition, where hybrids that feature a memantine-like unsubstituted amino group are significantly more potent that those with the linker attached at that amino group. However, for hAChE inhibition and NMDA antagonism, the linkage position does not have a clear effect, with the potencies depending on tether length and/or the presence of a basic bridgehead nitrogen atom. The novel hybrids are particularly potent on hAChE (IC_{50} in the 0.33–1.96 nM range) and then on hBChE (IC_{50} in the 0.021–2.36 μM range) and NMDA receptors (IC_{50} in the 0.89–8.29 μM range), but they seem to be devoid of activity on proteins other than their primary biological targets, showing weak inhibitory activity on Aβ42 and tau aggregation and BACE-1.

The increased potencies of all or some of the new hybrids relative to the parent compounds from which they were designed suggests that both pharmacophoric moieties are positively contributing to the interactions with all the primary targets. Indeed, all hybrids are clearly more potent hAChE inhibitors (up to 44-fold) than the parent 6-chlorotacrine (IC_{50} 14.5 nM), and some of them are also more potent for hBChE inhibition (up to 24-fold) than 6-chlorotacrine (IC_{50} 0.50 μM) and up to 2-fold more potent NMDA antagonists than the parent fluorobenzohomoadamantanamine **6** (IC_{50} 1.93 μM) and memantine (IC_{50} 1.50 μM). Overall, the most interesting benzohomoadamantane–chlorotacrine hybrids, **13b**, **18a**, and **18b** compare well with previously reported memantine– and amantadine–AChE inhibitor hybrids such as **3**-**5** (Figure 1), in terms of AChE inhibition and NMDA antagonism, and take on added value a nanomolar or submicromolar hBChE inhibitory activity, thereby constituting interesting leads for future multitarget anti-Alzheimer drug discovery programs.

4. Experimental part

4.1. Chemistry. General methods.

All reagents were obtained from commercial suppliers (Sigma Aldrich, Acros, Cymit) unless otherwise stated, and used without further purification. The reactions were monitored by thin-layer chromatography (TLC) using aluminium-backed sheets with silica gel 60 F_{254} (Merck, ref 1.05554). The spots were visualized by UV irradiation and / or 1% aq. $KMnO_4$, followed by charring with a heat-gun. Column chromatography was performed on silica gel 60 AC.C (35−70 mesh, SDS, ref 2000027). Melting points were determined in open capillary tubes with a MFB 595010M Gallenkamp melting point apparatus. IR spectra were run on a Perkin Elmer Spectrum RX I spectrophotometer. Absorption values are expressed as wavenumbers (cm^{-1}); only significant absorption bands are given. 400 MHz ^1H/ 100.6 MHz ^{13}C NMR spectra were recorded on a Varian Mercury 400 spectrometer, at the Centres Científics i Tecnologics of the University of Barcelona (CCiTUB). The chemical shifts are reported in ppm (δ scale) relative to solvent signals (CD_3OD at 3.31 and 49.0 ppm in the ^1H and ^{13}C NMR spectra, respectively; $CDCl_3$ at 7.26 and 77.00 ppm in the ^1H and ^{13} C NMR spectra, respectively), and coupling constants are reported in Hertz (Hz). Assignments given for the NMR spectra of the new compounds have been carried out by comparison with the NMR data of compounds **12b**, **13b**, and **18b**, which in turn, were assigned on the basis of COSY $^1H/^1H$ (standard procedures) and COSY $^1H/^{13}C$ (gHSQC and gHMBC sequences) experiments. High resolution mass spectra were carried out at the CCiTUB with a LC/MSD TOF Agilent Technologies spectrometer.

*4.1.1. 5-[(6-Chloro-1,2,3,4-tetrahydroacridin-9-yl)amino]-1-pentanol (**9b**)*

A mixture of 6,9-dichloro-1,2,3,4-tetrahydroacridine, **8** (1.50 g, 5.95 mmol) and 5-amino-1-pentanol (7.76 mL, 7.36 g, 71.3 mmol) was stirred at 135 ºC for 1 day. The mixture was cooled to room temperature, poured onto water (200 mL), diluted with 5N NaOH (50 mL), and extracted with EtOAc (3 × 100 mL). The combined organic extracts were dried over anhydrous Na_2SO_4 and evaporated at reduced pressure, to give a dark brown oily residue (2.50 g), which was purified through column chromatography (35–70 μm silica gel, CH_2Cl_2 /MeOH / 50% aq. NH_4OH mixtures, gradient elution). On elution with CH_2Cl_2 /MeOH / 50% aq. NH_4OH 97:3:0.4, alcohol **9b** (767 mg, 40% yield) was isolated as a yellow solid; R_f 0.32 (CH_2Cl_2 / MeOH / 50% aq. NH_4OH 95:5:1).

A solution of **9b** (55 mg, 0.17 mmol) in CH_2Cl_2 (1 mL) was filtered through a 0.2 μm PTFE filter, treated with a methanolic solution of HCl (0.5 M, 1.0 mL), and evaporated at reduced pressure. The solid was washed with pentane (3 × 2 mL) to give, after drying at 65 ºC / 2 Torr for 48 h, **9b**·HCl (61 mg) as a beige solid: mp 148–150 °C; IR (ATR) *ν* 3400–2400 (max at 3250, 2924, 2859, O–H, N–H, $^+$N–H, C–H st), 1629, 1567, 1513 (Ar–C–C, Ar–C–N st) cm^{-1}; ^{1}H NMR (400 MHz, CD_3OD) *δ* 1.51 (m, 2H, 3-H_2), 1.67 (m, 2H, 2-H_2), 1.88 (m, 2H, 4-H_2), 1.92–2.20 (m, 4H, 2'-H_2, 3'-H_2), 2.68 (t, *J* = 6.0 Hz, 2H, 1'-H_2), 3.00 (t, *J* = 6.0 Hz, 2H, 4'-H_2), 3.57 (t, *J* = 6.4 Hz, 2H, 1-H_2), 3.96 (t, *J* = 7.2 Hz, 2H, 5-H_2), 4.85 (s, $^+$NH, NH, OH), 7.57 (dd, *J* = 9.2 Hz, *J'* = 2.0 Hz, 1H, 7'-H), 7.77 (d, *J* = 2.0 Hz, 1H, 5'-H), 8.40 (d, *J* = 9.2 Hz, 1H, 8'-H); ^{13}C NMR (100.6 MHz, CD_3OD) *δ* 21.8 (CH_2, C3'), 22.9 (CH_2, C2'), 24.1 (CH_2, C3), 24.7 (CH_2, C1'), 29.3 (CH_2, C4'), 31.1 (CH_2, C4), 33.0 (CH_2, C2), 48.8 (CH_2, C5), 62.6 (CH_2, C1), 113.4 (C, C9a'), 115.4 (C, C8a'), 119.1 (CH, C5'), 126.8 (CH, C7'), 128.8 (CH, C8'), 140.1 (C, C6'), 140.5 (C, C10a'), 152.1 (C, C4a'), 157.9 (C, C9'); HRMS (ESI), calcd for [$C_{18}H_{23}{}^{35}ClN_2O$ + H^+] 319.1578, found 319.1585.

*4.1.2. 5-[(6-Chloro-1,2,3,4-tetrahydroacridin-9-yl)amino]pentyl methanesulfonate (**10b**)*

A solution of alcohol **9b** (368 mg, 1.15 mmol) and anhydrous Et_3N (0.27 mL, 197 mg, 1.95 mmol) in dry CH_2Cl_2 (7 mL) was cooled at –10 °C with an ice / NaCl bath, and, then, treated dropwise with methanesulfonyl chloride (0.13 mL, 192 mg, 1.68 mmol). The reaction mixture was stirred at –10 °C for 30 min and concentrated in vacuo. The residue was taken up in CH_2Cl_2 (20 mL), washed with 2N NaOH (3 × 15 mL), dried over anhydrous Na_2SO_4, and evaporated at reduced pressure, to afford mesylate **10b** (461 mg, quantitative yield) as a dark brown oil; R_f 0.72 (CH_2Cl_2 / MeOH / 50% aq. NH_4OH 95:5:1).

A solution of **10b** (25 mg, 0.06 mmol) in CH_2Cl_2 (1 mL) was filtered through a 0.2 μm PTFE filter and evaporated *in vacuo*. The resulting solid was washed with pentane (3 × 2 mL), to afford, after drying at 65 ºC / 2 Torr for 48 h, the analytical sample of **10b** (24 mg) as a dark brown oil; IR (ATR) *ν* 3286 (N–H st), 1634, 1604, 1574, 1555 (Ar–C–C, Ar–C–N st) cm^{-1}; ^{1}H NMR (400 MHz, $CDCl_3$) *δ* 1.54 (m, 2H, 3-H_2), 1.70–1.84 (m, 4H, 2-H_2, 4-H_2), 1.86–1.93 (m, 4H, 2'-H_2, 3'-H_2), 2.67 (t, 2H, 1'-H_2), 2.99 (s, 3H, CH_3SO_3), 3.03 (m, 2H, 4'-H_2), 3.58 (m, 2H, 5-H_2), 4.24 (t, *J* = 6.4 Hz, 2H, 1-H_2), 7.25 (dd, *J* = 9.2 Hz, *J'* = 2.0 Hz, 1H, 7'-H), 7.88 (d, *J* = 2.0 Hz, 1H, 5'-H),

7.93 (d, J = 9.2 Hz, 1H, 8'-H); ^{13}C NMR (100.6 MHz, $CDCl_3$, this compound decomposed partially during acquisition of the spectrum, only some representative signals are given) δ 22.1 (CH_2), 22.7 (CH_2), 22.8 (CH_2) (C3, C2', C3'), 24.7 (CH_2, C1'), 28.8 (CH_2, C4), 30.9 (CH_2, C2), 32.6 (CH_2, C4'), 37.4 (CH_3, OSO_2CH_3), 48.8 (CH_2, C5), 69.5 (CH_2, C1), 114.9 (C, C9a'), 117.5 (C, C8a'), 151.7 (C, C4a'), 157.9 (C, C9'); HRMS (ESI), calcd for [$C_{19}H_{25}{}^{35}ClN_2O_3$ + H^+] 397.1347, found 397.1353.

*4.1.3. 4-[(6-Chloro-1,2,3,4-tetrahydroacridin-9-yl)amino]butanenitrile (**11a**)*

A mixture of mesylate **10a** [58] (2.32 g, 5.58 mmol) and NaCN (1.64 g, 33.5 mmol) in dry DMF (5 mL) was stirred at 100 °C for 1 h, neutralized with 1N NaOH (50 mL), and extracted with CH_2Cl_2 (4 × 30 mL). The combined organic extracts were washed with water (6 × 40 mL), dried over anhydrous Na_2SO_4, and evaporated under reduced pressure, to give nitrile **11a** (1.61 g, 98% yield) as a brown oil; R_f 0.68 (CH_2Cl_2 / MeOH / 50% aq. NH_4OH 95:5:1).

A solution of **11a** (142 mg, 0.47 mmol) in CH_2Cl_2 (1 mL) was filtered through a 0.2 μm PTFE filter, treated with a methanolic solution of HCl (0.5 M, 0.8 mL), and evaporated at reduced pressure. The solid was washed with pentane (3 × 2 mL) to give, after drying at 65 ºC / 2 Torr for 48 h, **11a**·HCl (154 mg) as a brown solid: mp 114–116 °C; IR (ATR) ν 3500–2500 (max at 3050, 2930, 2861, 2761, N–H, $^+$N–H, C–H st), 2232 (CN st), 1629, 1567, 1514 (Ar–C–C, Ar–C–N st) cm^{-1}; ^{1}H NMR (400 MHz, CD_3OD) δ 1.92–2.02 (m, 4H, 2'-H_2, 3'-H_2), 2.18 (tt, J = J' = 7.2 Hz, 2H, 3-H_2), 2.62 (t, J = 7.2 Hz, 2H, 2-H_2), 2.73 (t, J = 6.0 Hz, 2H, 1'-H_2), 3.02 (t, J = 5.6 Hz, 2H, 4'-H_2), 4.08 (t, J = 7.2 Hz, 2H, 4-H_2), 4.85 (s, $^+$NH, NH), 7.58 (dd, J = 9.2 Hz, J' = 2.0 Hz, 1H, 7'-H), 7.80 (d, J = 2.0 Hz, 1H, 5'-H), 8.39 (d, J = 9.2 Hz, 1H, 8'-H); ^{13}C NMR (100.6 MHz, CD_3OD) δ 15.1 (CH_2, C2), 21.7 (CH_2, C3'), 22.9 (CH_2, C2'), 25.0 (CH_2, C1'), 27.1 (CH_2, C3), 29.4 (CH_2, C4'), 47.8 (CH_2, C4), 113.9 (C, C9a'), 115.5 (C, C8a'), 119.2 (CH, C5'), 120.5 (C, C1), 127.1 (CH, C7'), 128.6 (CH, C8'), 140.2 (C, C6'), 140.4 (C, C10a'), 152.6 (C, C4a'), 157.9 (C, C9'); HRMS (ESI), calcd for [$C_{17}H_{18}{}^{35}ClN_3$ + H^+] 300.1262, found 300.1265.

*4.1.4. 5-[(6-Chloro-1,2,3,4-tetrahydroacridin-9-yl)amino]pentanenitrile (**11b**)*

A mixture of 6-chlorotacrine, **7** (1.50 g, 6.45 mmol), finely powdered KOH (85% purity, 851 mg, 12.9 mmol), and 4 Å molecular sieves in dry DMSO (20 mL) was stirred, heating every 10 min with a heat gun for 1 h, and at room temperature for 1

additional h, and it was then treated with 5-bromovaleronitrile (0.9 mL, 1.25 g, 7.71 mmol). The reaction mixture was stirred at room temperature overnight, then diluted with 5N NaOH (350 mL), and extracted with EtOAc (3 × 150 mL). The combined organic extracts were washed with water (3 × 200 mL), dried over anhydrous Na_2SO_4, and evaporated under reduced pressure, to give a yellow oily residue (2.28 g), which was subjected to column chromatography purification (35−70 μm silica gel, CH_2Cl_2 / 50% aq. NH_4OH 100:0.4), to afford nitrile **11b** (1.30 g, 64% yield) as a light yellow solid; R_f 0.73 (CH_2Cl_2 / MeOH / 50% aq. NH_4OH 95:5:1).

A solution of **11b** (21 mg, 0.07 mmol) in CH_2Cl_2 (1 mL) was filtered through a 0.2 μm PTFE filter, treated with a methanolic solution of HCl (0.5 M, 0.4 mL), and evaporated at reduced pressure. The solid was washed with pentane (3 × 2 mL) to give, after drying at 65 ºC / 2 Torr for 48 h, **11b**·HCl (35 mg) as a yellow solid: mp 73–75 °C; IR (ATR) *v* 3500–2500 (max at 3126, 3043, 2920, 2857, N–H, $^+$N–H, C–H st), 2236 (CN st), 1631, 1573, 1515 (Ar–C–C, Ar–C–N st) cm^{-1}; ^{1}H NMR (400 MHz, CD_3OD) δ 1.78 (m, 2H, 3-H_2), 1.92–2.02 (m, 6H, 4-H_2, 2'-H_2, 3'-H_2), 2.54 (t, J = 6.0 Hz, 2H, 2-H_2), 2.70 (t, 2H, 1'-H_2), 3.00 (t, 2H, 4'-H_2), 4.00 (t, J = 7.2 Hz, 2H, 5-H_2), 4.85 (s, $^+$NH, NH), 7.57 (dd, J = 9.2 Hz, J' = 2.0 Hz, 1H, 7'-H), 7.78 (d, J = 2.0 Hz, 1H, 5'-H), 8.39 (d, J = 9.2 Hz, 1H, 8'-H); ^{13}C NMR (100.6 MHz, CD_3OD) δ 17.5 (CH_2, C2), 21.9 (CH_2, C3'), 23.0 (CH_2, C2'), 24.1 (CH_2, C3), 25.2 (CH_2, C1'), 29.6 (CH_2, C4'), 30.6 (CH_2, C4), 49.9 (CH_2, C5), 113.7 (C, C9a'), 115.6 (C, C8a'), 119.3 (CH, C5'), 120.9 (C, C1), 127.1 (CH, C7'), 128.9 (CH, C8'), 140.1 (C, C6'), 140.5 (C, C10a'), 152.4 (C, C4a'), 157.9 (C, C9'); HRMS (ESI), calcd for [$C_{18}H_{20}{}^{35}ClN_3$ + H^+] 314.1419, found 314.1416.

*4.1.5. 4-[(6-Chloro-1,2,3,4-tetrahydroacridin-9-yl)amino]-N-(9-fluoro-7H-5,6,8,9,10,11-hexahydro-5,9:7,11-dimethanobenzo[9]annulen-7-yl)butanamide (**12a**)*

A solution of nitrile **11a** (1.53 g, 5.20 mmol) in MeOH (6.5 mL) was treated with a 40% methanolic solution of KOH (13 mL). The resulting suspension was stirred under reflux for 3 h, then treated with water (21 mL), and again stirred under reflux overnight. The resulting solution was cooled to room temperature and evaporated in vacuo. The resulting residue was treated with HCl / Et_2O (0.73 N, 142 mL), and the mixture was concentrated *in vacuo* to give the corresponding carboxylic acid in the form of hydrochloride salt (7.42 g), which was used in the following step without further purification.

To a suspension of crude carboxylic acid (1.94 g of a crude that could contain a maximum of 1.36 mmol of the carboxylic acid) in a mixture of EtOAc (25 mL) and DMF (2 mL), *N*-(3-dimethylaminopropyl)-*N'*-ethylcarbodiimide hydrochloride (EDC hydrochloride) (316 mg, 1.65 mmol), Et_3N (0.94 mL, 685 mg, 6.78 mmol), and 1-hydroxy-1*H*-benzotriazole (HOBt) (185 mg, 1.36 mmol) were added. The resulting mixture was stirred at room temperature for 15 min, and then treated with a suspension of amine **6** (346 mg, 1.50 mmol) in a mixture of EtOAc (16 mL) and DMF (2 mL). The reaction mixture was stirred at room temperature for 2 days, then concentrated *in vacuo*, diluted with 1N NaOH (200 mL), and extracted with CH_2Cl_2 (2 × 150 mL). The combined organic extracts were washed with water (5 × 100 mL), dried over anhydrous Na_2SO_4, and evaporated under reduced pressure to give a brown oil (696 mg), which was subjected to column chromatography purification (35−70 μm silica gel, CH_2Cl_2 / MeOH / 50% aq. NH_4OH mixtures, gradient elution). On elution with CH_2Cl_2 / MeOH / 50% aq. NH_4OH 99.8:0.2:0.4, amide **12a** (288 mg, 40% yield) was isolated as a brown oil; R_f 0.53 (CH_2Cl_2 / MeOH / 50% aq. NH_4OH 95:5:1).

A solution of **12a** (26 mg, 0.05 mmol) in CH_2Cl_2 (1 mL) was filtered through a 0.2 μm PTFE filter, treated with a methanolic solution of HCl (0.5 M, 0.3 mL), and evaporated at reduced pressure. The solid was washed with pentane (3 × 2 mL) to give, after drying at 65 ºC / 2 Torr for 48 h, **12a**·HCl (27 mg) as a yellow solid: mp 169–173 ºC; IR (ATR) *ν* 3500–2400 (max at 3246, 3054, 2917, 2852, 2795, N–H, $^+$N–H, C–H st), 1631, 1584, 1574 (C=O, Ar–C–C, Ar–C–N st) cm^{-1}; ^1H NMR (400 MHz, CD_3OD) δ 1.80 [br d, J = 10.8 Hz, 2H, 10"(13")-H_A], 1.90–1.95 (m, 4H, 2'-H_2, 3'-H_2), 1.98–2.17 [m, 10H, 3-H_2, 6"(12")-H_A, 6"(12")-H_B, 10"(13")-H_B, 8"-H_2], 2.37 (t, J = 6.4 Hz, 2H, 2-H_2), 2.69 (br signal, 2H, 1'-H_2), 2.97 (br signal, 2H, 4'-H_2), 3.21 [m, 2H, 5"(11")-H], 3.97 (t, J = 6.4 Hz, 2H, 4-H_2), 4.86 (s, $^+$NH, NH), 7.06–7.14 [m, 4H, 1"(4")-H, 2"(3")-H], 7.49 (dd, J = 9.2 Hz, J' = 2.0 Hz, 1H, 7'-H), 7.75 (d, J = 2.0 Hz, 1H, 5'-H), 8.41 (d, J = 9.2 Hz, 1H, 8'-H); ^{13}C NMR (100.6 MHz, CD_3OD) δ 21.8 (CH_2, C3'), 22.8 (CH_2, C2'), 25.0 (CH_2, C1'), 26.5 (CH_2, C3), 29.3 (CH_2, C4'), 34.8 (CH_2, C2), 39.3 [CH_2, d, $J_{C\text{-}F}$ = 1.3 Hz, C6"(12")], 40.9 [CH, d, $J_{C\text{-}F}$ = 12.9 Hz, C5"(11")], 41.3 [CH_2, d, $J_{C\text{-}F}$ = 20.0 Hz, C10"(13")], 46.9 (CH_2, d, $J_{C\text{-}F}$ = 18.1 Hz, C8"), 49.3 (CH_2, C4), 58.8 (C, d, $J_{C\text{-}F}$ = 11.0 Hz, C7"), 94.7 (C, d, $J_{C\text{-}F}$ = 176.8 Hz, C9"), 113.4 (C, C9a'), 115.4 (C, C8a'), 119.0 (CH, C5'), 126.7 (CH, C7'), 128.0 [CH, C2"(3")], 129.0 (CH, C8'), 129.1 [CH, C1"(4")], 140.1 (C, C6'), 140.5 (C, C10a'), 146.2 [C, C4a"(11a")], 151.9 (C, C4a'),

157.9 (C, C9'), 174.4 (C, C1); HRMS (ESI), calcd for [$C_{32}H_{35}{}^{35}ClFN_3O + H^+$] 532.2525, found 532.2525.

*4.1.6. 5-[(6-Chloro-1,2,3,4-tetrahydroacridin-9-yl)amino]-N-(9-fluoro-7H-5,6,8,9,10,11-hexahydro-5,9:7,11-dimethanobenzo[9]annulen-7-yl)pentanamide (**12b**)*

This compound was prepared as described for **12a**. From nitrile **11b** (1.24 g, 4.04 mmol), crude carboxylic acid (6.17 g) was obtained as the hydrochloride salt and used in the following step without further purification. From crude carboxylic acid (1.21 g of a crude that could contain a maximum of 0.79 mmol of carboxylic acid) and amine **6** (200 mg, 0.87 mmol), a brown solid residue (1.87 g) was obtained and subjected to column chromatography purification (35−70 μm silica gel, CH_2Cl_2 / MeOH / 50% aq. NH_4OH mixtures, gradient elution). On elution with CH_2Cl_2 / MeOH / 50% aq. NH_4OH 99:1:0.4 to 98.5:1.5:0.4, amide **12b** (324 mg, 75% yield) was isolated as a yellow oil; R_f 0.61 (CH_2Cl_2 / MeOH / 50% aq. NH_4OH 95:5:1).

A solution of **12b** (36 mg, 0.07 mmol) in CH_2Cl_2 (1 mL) was filtered through a 0.2 μm PTFE filter, treated with a methanolic solution of HCl (0.5 M, 0.4 mL), and evaporated at reduced pressure. The solid was washed with pentane (3 × 2 mL) to give, after drying at 65 ºC / 2 Torr for 48 h, **12b**·HCl (38 mg) as a yellow solid: mp 181–185 ºC; IR (ATR) *v* 3500–2500 (max at 3193, 3126, 3043, 2915, 2857, N–H, $^+$N–H, C–H st), 1632, 1589, 1571 (C=O, Ar–C–C, Ar–C–N st) cm^{-1}; ^1H NMR (400 MHz, CD_3OD) δ 1.68 (m, 2H, 3-H_2), 1.77–1.85 [m, 4H, 4-H_2,10"(13")-H_A], 1.91–1.95 (m, 4H, 2'-H_2, 3'-H_2), 1.98–2.15 [m, 8H, 6"(12")-H_A, 6"(12")-H_B, 10"(13")-H_B, 8"-H_2], 2.20 (t, J = 6.8 Hz, 2H, 2-H_2), 2.67 (br signal, 2H, 1'-H_2), 2.98 (br signal, 2H, 4'-H_2), 3.20 [m, 2H, 5"(11")-H], 3.94 (t, J = 6.8 Hz, 2H, 5-H_2), 4.85 (s, $^+$NH, NH), 7.06–7.13 [m, 4H, 1"(4")-H, 2"(3")-H], 7.53 (dd, J = 9.2 Hz, J' = 2.4 Hz, 1H, 7'-H), 7.76 (d, J = 2.4 Hz, 1H, 5'-H), 8.39 (d, J = 9.2 Hz, 1H, 8'-H); ^{13}C NMR (100.6 MHz, CD_3OD) δ 21.7 (CH_2, C3'), 22.8 (CH_2, C2'), 23.6 (CH_2, C3), 24.8 (CH_2, C1'), 29.3 (CH_2, C4'), 30.5 (CH_2, C4), 36.7 (CH_2, C2), 39.3 [CH_2, d, $J_{C\text{-}F}$ = 2.0 Hz, C6"(12")], 40.9 [CH, d, $J_{C\text{-}F}$ = 12.9 Hz, C5"(11")], 41.3 [CH_2, d, $J_{C\text{-}F}$ = 20.0 Hz, C10"(13")], 46.8 (CH_2, d, $J_{C\text{-}F}$ = 18.1 Hz, C8"), 48.8 (CH_2, C5), 58.7 (C, d, $J_{C\text{-}F}$ = 11.6 Hz, C7"), 94.7 (C, d, $J_{C\text{-}F}$ = 176.8 Hz, C9"), 113.5 (C, C9a'), 115.5 (C, C8a'), 119.1 (CH, C5'), 126.8 (CH, C7'), 128.0 [CH, C2"(3")], 128.8 (CH, C8'), 129.1 [CH, C1"(4")], 140.1 (C, C6'), 140.5 (C, C10a'),

146.2 [C, C4a"(11a")], 152.1 (C, C4a'), 157.8 (C, C9'), 174.8 (C, C1); HRMS (ESI), calcd for [$C_{33}H_{37}{}^{35}ClFN_3O + H^+$] 546.2682, found 546.2685.

*4.1.7. N-(6-Chloro-1,2,3,4-tetrahydroacridin-9-yl)-N'-(9-fluoro-7H-5,6,8,9,10,11-hexahydro-5,9:7,11-dimethanobenzo[9]annulen-7-yl)-1,4-butanediamine (**13a**)*

A solution of amide **12a** (124 mg, 0.22 mmol) in dry THF (5 mL) was cooled to 0 °C with an ice bath, and then treated dropwise with BH_3·THF (1M in THF, 0.87 mL, 0.87 mmol). The reaction mixture was stirred at room temperature overnight. The resulting mixture was cooled to 0 °C, and treated dropwise with MeOH (3 mL) and water (3 mL). The organic phase was evaporated under reduced pressure, and the aqueous phase was diluted with 1N NaOH (10 mL) and extracted with CH_2Cl_2 (3 × 10 mL). The combined organic extracts were dried over anhydrous Na_2SO_4 and evaporated *in vacuo*, to give a beige solid residue (111 mg), which was subjected to column chromatography purification (35−70 μm silica gel, hexane / EtOAc / 50% aq. NH_4OH mixtures, gradient elution). On elution with hexane / EtOAc / 50% aq. NH_4OH 50:50:0.4, starting **12a** (41 mg) was recovered. On elution with hexane / EtOAc / 50% aq. NH_4OH 40:60:0.4, amine **13a** (27 mg, 24% yield) was isolated as a yellow sticky solid; R_f 0.45 (CH_2Cl_2 / MeOH / 50% aq. NH_4OH 95:5:1).

A solution of **13a** (27 mg, 0.05 mmol) in CH_2Cl_2 (1 mL) was filtered through a 0.2 μm PTFE filter, treated with a methanolic solution of HCl (0.5 M, 0.3 mL), and evaporated at reduced pressure. The solid was washed with pentane (3 × 2 mL) and recrystallized from MeOH / EtOAc 1:1 (1 mL), to give, after drying at 65 ºC / 2 Torr for 48 h, the analytical sample of **13a**·2HCl (7 mg), as a pale yellow solid: ^{1}H NMR (400 MHz, CD_3OD) δ 1.81 (m, 2H, 2-H_2), 1.86–2.03 (m, 10H, 3-H_2, 2'-H_2, 3'-H_2, 6"(12")-H_A, 10"(13")-H_A], 2.14–2.26 [m, 6H, 6"(12")-H_B, 10"(13")-H_B, 8"-H_2], 2.71 (m, 2H, 1'-H_2), 3.00 (m, 2H, 4'-H_2), 3.08 (t, J = 7.6 Hz, 2H, 1-H_2), 3.41 [m, 2H, 5"(11")-H], 4.01 (t, J = 7.2 Hz, 2H, 4-H_2), 4.85 (s, $^+$NH, NH), 7.16 [m, 4H, 1"(4")-H, 2"(3")-H], 7.58 (dd, J = 8.8 Hz, J' = 2.0 Hz, 1H, 7'-H), 7.77 (d, J = 2.0 Hz, 1H, 5'-H), 8.41 (d, J = 8.8 Hz, 1H, 8'-H); ^{13}C NMR (100.6 MHz, CD_3OD) δ 21.7 (CH_2, C3'), 22.9 (CH_2, C2'), 24.9 (CH_2, C1'), 25.1 (CH_2, C3), 28.5 (CH_2, C2), 29.4 (CH_2, C4'), 36.6 [CH_2, C6"(12")], 40.0 [CH, d, $J_{C\text{-}F}$ = 13.1 Hz, C5"(11")], 40.7 [CH_2, d, $J_{C\text{-}F}$ = 20.1 Hz, C10"(13")], 41.2 (CH_2, C1), 44.4 (CH_2, d, $J_{C\text{-}F}$ = 21.1 Hz, C8"), 49.7 (CH_2, C4), 63.8 (C, d, $J_{C\text{-}F}$ = 11.1 Hz, C7"), 94.2 (C, d, $J_{C\text{-}F}$ = 180.1 Hz, C9"), 113.8 (C, C9a'), 115.6 (C, C8a'), 119.2 (CH, C5'), 127.0 (CH, C7'), 128.6 [CH, C2"(3")], 128.7 (CH, C8'), 129.4 [CH, C1"(4")], 140.1 (C,

C6'), 140.6 (C, C10a'), 145.1 [C, C4a"(11a")], 152.5 (C, C4a'), 157.9 (C, C9'); HRMS (ESI), calcd for [$C_{32}H_{37}{}^{35}ClFN_3 + H^+$] 518.2733, found 518.2710.

*4.1.8. N-(6-Chloro-1,2,3,4-tetrahydroacridin-9-yl)-N'-(9-fluoro-7H-5,6,8,9,10,11-hexahydro-5,9:7,11-dimethanobenzo[9]annulen-7-yl)-1,5-pentanediamine (**13b**)*

4.1.8.1. From **12b**. This compound was prepared as decribed for **13a**. From amide **12b** (100 mg, 0.18 mmol), an orange solid residue (79 mg) was obtained and subjected to column chromatography purification (35−70 μm silica gel, hexane / EtOAc / Et_3N mixtures, gradient elution). On elution with hexane / EtOAc / Et_3N 30:70:0.2, amine **13b** (10 mg, 10% yield) was isolated as a yellow solid; R_f 0.45 (CH_2Cl_2 / MeOH / 50% aq. NH_4OH 95:5:1).

A solution of **13b** (10 mg, 0.02 mmol) in CH_2Cl_2 (1 mL) was filtered through a 0.2 μm PTFE filter, treated with a methanolic solution of HCl (1.35 M, 0.13 mL), and evaporated at reduced pressure. The solid was washed with pentane (3 × 2 mL), to give, after drying at 65 ºC / 2 Torr for 48 h, the analytical sample of **13b**·2HCl (12 mg), as a yellow solid: ^{1}H NMR (400 MHz, CD_3OD) δ 1.55 (tt, $J = J' = 7.6$ Hz, 2H, 3-H_2), 1.77 (tt, $J = J' = 7.6$ Hz 2H, 2-H_2), 1.85–1.99 [m, 10H, 4-H_2, 2'-H_2, 3'-H_2, 6"(12")-H_A, 10"(13")-H_A], 2.16–2.26 [m, 6H, 6"(12")-H_B, 10"(13")-H_B, 8"-H_2], 2.70 (m, 2H, 1'-H_2), 3.00 (m, 2H, 4'-H_2), 3.04 (t, $J = 7.6$ Hz, 2H, 1-H_2), 3.41 [m, 2H, 5"(11")-H], 3.97 (t, $J = 7.6$ Hz, 2H, 5-H_2), 4.85 (s, $^+$NH, NH), 7.15 [m, 4H, 1"(4")-H, 2"(3")-H], 7.57 (dd, $J = 9.6$ Hz, $J' = 2.0$ Hz, 1H, 7'-H), 7.78 (d, $J = 2.0$ Hz, 1H, 5'-H), 8.41 (d, $J = 9.6$ Hz, 1H, 8'-H); ^{13}C NMR (100.6 MHz, CD_3OD) δ 21.7 (CH_2, C3'), 22.9 (CH_2, C2'), 24.8 (2 CH_2, C1', C3), 27.4 (CH_2, C2), 29.3 (CH_2, C4'), 30.8 (CH_2, C4), 36.5 [CH_2, C6"(12")], 40.0 [CH, d, $J_{C\text{-}F} = 13.0$ Hz, C5"(11")], 40.7 [CH_2, d, $J_{C\text{-}F} = 20.6$ Hz, C10"(13")], 41.3 (CH_2, C1), 44.3 (CH_2, d, $J_{C\text{-}F} = 20.7$ Hz, C8"), 49.2 (CH_2, C5), 63.7 (C, d, $J_{C\text{-}F} = 11.0$ Hz, C7"), 94.2 (C, d, $J_{C\text{-}F} = 180.0$ Hz, C9"), 113.5 (C, C9a'), 115.5 (C, C8a'), 119.1 (CH, C5'), 126.9 (CH, C7'), 128.5 [CH, C2"(3")], 128.8 (CH, C8'), 129.4 [CH, C1"(4")], 140.1 (C, C6'), 140.5 (C, C10a'), 145.2 [C, C4a"(11a")], 152.2 (C, C4a'), 157.9 (C, C9'); HRMS (ESI), calcd for [$C_{33}H_{39}{}^{35}ClFN_3 + H^+$] 532.2889, found 532.2906.

4.1.8.2. From **10b**. A solution of mesylate **10b** (237 mg, 0.60 mmol) in DMF (1.5 mL) was added to a stirred suspension of amine **6** (115 mg, 0.42 mmol) and K_2CO_3 (130 mg, 0.94 mmol) in DMF. The reaction mixture was stirred at 80 ºC for 2 days and then it was concentrated *in vacuo*. The resulting residue was taken up in water (15 mL) and 2N

NaOH (15 mL), and extracted with CH_2Cl_2 (3×20 mL). The combined organic extracts were dried over anhydrous Na_2SO_4 and evaporated at reduced pressure, to give a dark brown oil (309 mg), which was subjected to column chromatography purification (35−70 μm silica gel, CH_2Cl_2 / MeOH / 50% aq. NH_4OH mixtures, gradient elution). On elution with CH_2Cl_2 / MeOH / 50% aq. NH_4OH 98.6:1.4:0.4, byproduct 6-chloro-9-(5-chloropentylamino)-1,2,3,4-tetrahydroacridine (38 mg) was isolated. On elution with CH_2Cl_2 / MeOH / 50% aq. NH_4OH 97:3:0.4, an inseparable 1.5:1 mixture of the desired amide **13b** and byproduct 5-[(6-chloro-1,2,3,4-tetrahydroacridin-9-yl)amino]-1-pentanol (86 mg, 27% yield of **13b**) was obtained.

*4.1.9. tert-Butyl (9-fluoro-7H-5,6,8,9,10,11-hexahydro-2-nitro-5,9:7,11-dimethanobenzo[9]annulen-7-yl)carbamate (**15**)*

To a mixture of amine **14** [59] (496 mg, 1.79 mmol) and 2N NaOH (1.4 mL) in THF (3.5 mL), di-*tert*-butyl dicarbonate (355 mg, 1.62 mmol) was added. The reaction mixture was stirred at room temperature for 16 h, then cooled in an ice bath, neutralized with 2N HCl, and extracted with EtOAc. The combined organic extracts were dried over anhydrous Na_2SO_4 and evaporated *in vacuo*, to give the *N*-Boc protected amine **15** (589 mg, 87% yield): mp 204–205 ºC; IR (NaCl) *v* 3426 (N–H st), 1725, 1714 (C=O st), 1608, 1588, 1520, 1505 (NO_2 st as), 1391, 1360, 1345, 1306, 1285 (NO_2 st s) cm^{-1}; ^1H NMR (400 MHz, $CDCl_3$) δ 1.41 [s, 9H, $C(CH_3)_3$], 1.88–2.24 (m, 10H, methylene protons), 3.37 (m, 2H, 5-H, 11-H), 4.58 (br.s., 1H, NHCOO), 7.25 (dd, J = 7.2 Hz, J' = 2.0 Hz, 1H, 3-H), 7.97–8.00 (m, 2H, 1-H, 4-H); ^{13}C NMR (100.6 MHz, $CDCl_3$) δ 28.5 [CH_3, $C(CH_3)_3$], 38.2 (CH_2), 38.5 (CH_2) (C6, C12), 39.51 (CH, d, J_{C-F} = 13.3 Hz), 39.59 (CH, d, J_{C-F} = 13.3 Hz) (C5, C11), 39.55 (CH_2, d, J_{C-F} = 21.3 Hz), 39.8 (CH_2, d, J_{C-F} = 20.7 Hz) (C10, C13), 46.1 (CH_2, d, J_{C-F} = 18.2 Hz, C8), 56.3 (C, d, J_{C-F} = 11.3 Hz, C7), 79.8 (C, $C(CH_3)_3$], 93.6 (C, d, J_{C-F} = 178.5 Hz, C9), 122.3 (CH), 123.3 (CH) (C1, C4), 129.4 (CH, C3), 146.3 (C), 146.9 (C) (C4a, C11a), 152.4 (C, C2), 154.1 (C, NHCOO); HRMS (ESI), calcd for [$C_{20}H_{25}FN_2O_4 - H^-$] 375.1726, found 375.1738.

*4.1.10. tert-Butyl (2-amino-9-fluoro-7H-5,6,8,9,10,11-hexahydro-5,9:7,11-dimethanobenzo[9]annulen-7-yl)carbamate (**16**)*

A suspension of the nitro derivative **15** (583 mg, 1.54 mmol) and PtO_2 (48 mg, 0.12 mmol) in EtOH (100 mL) was hydrogenated at 1 atm of H_2 at room temperature for 4 h. The resulting black suspension was filtered and the filtrate was evaporated at reduced

pressure to give amine **16** (495 mg, 92 % yield) as a yellow solid: mp 118–120 ºC; IR (NaCl) *v* 3411, 3363 (N–H st), 1713 (C=O st), 1616, 1586, 1505 (NO_2 st as), 1453, 1391, 1365, 1340, 1306, 1282 (NO_2 st s) cm^{-1}; ^1H NMR (400 MHz, $CDCl_3$) δ 1.42 [s, 9H, $C(CH_3)_3$], 1.83–2.20 (m, 10H, methylene protons), 3.06 (m, 1H), 3.11 (m, 1H) (5-H, 11-H), 3.24 (br.s., 1H), 3.90 (br.s., 1H) (2-NH_2), 4.51 (br.s., 1H, NHCOO), 6.427 (dd, J = 6.4 Hz, J' = 2.4 Hz, 1H, 3-H), 6.434 (d, J = 2.4 Hz, 1H, 1-H), 6.85 (d, J = 6.4 Hz, 1H, 4-H); ^{13}C NMR (100.6 MHz, $CDCl_3$) δ 28.6 [CH_3, $C(CH_3)_3$], 38.7 (CH, d, J_{C-F} = 13.3 Hz, C5), 38.9 (CH_2), 39.6 (CH_2) (C6, C12), 39.8 (CH, d, J_{C-F} = 13.5 Hz, C11), 40.2 (CH_2, d, J_{C-F} = 20.1 Hz), 40.7 (CH_2, d, J_{C-F} = 19.5 Hz) (C10, C13), 46.4 (CH_2, d, J_{C-F} = 17.1 Hz, C8), 56.6 (C, d, J_{C-F} = 11.5 Hz, C7), 79.4 [C, $C(CH_3)_3$], 94.6 (C, d, J_{C-F} = 177.0 Hz, C9), 113.1 (CH), 115.3 (CH (C1, C3), 129.3 (CH, C4), 135.2 (C, C2), 145.1 (C), 145.9 (C) (C4a, C11a), 154.1 (C, NHCOO); HRMS (ESI), calcd for [$C_{20}H_{27}FN_2O_2 + H^+$] 347.2129, found 347.2132.

*4.1.11. N-(7-Amino-9-fluoro-7H-5,6,8,9,10,11-hexahydro-5,9:7,11-dimethanobenzo[9]annulen-2-yl)-4-[(6-chloro-1,2,3,4-tetrahydroacridin-9-yl)amino]butanamide (**18a**)*

N-{7-[(*tert*-Butoxycarbonyl)amino]-9-fluoro-7*H*-5,6,8,9,10,11-hexahydro-5,9:7,11-dimethanobenzo[9]annulen-2-yl}-4-[(6-chloro-1,2,3,4-tetrahydroacridin-9-yl)amino]butanamide (**17a**) was prepared as described for **12a**. From nitrile **11a** (369 mg, 1.23 mmol), crude carboxylic acid (2.55 g) was obtained as the hydrochloride salt and used in the following step without further purification. From this crude carboxylic acid and amine **16** (302 mg, 0.87 mmol), a brown sticky solid residue (3.11 g) was obtained and subjected to column chromatography purification (35−70 μm silica gel, hexane / EtOAc / Et_3N mixtures, gradient elution). On elution with hexane / EtOAc / Et_3N 20:80:0.2 to 10:90.5:0.2, impure amide **17a** (235 mg) was isolated as a yellow oil and used in the following step without further purification; R_f 0.72 (CH_2Cl_2 / MeOH / 50% aq. NH_4OH 95:5:1); LRMS (ESI), 647.3159 ($M + H^+$).

A mixture of *N*-Boc-protected amide **17a** (218 mg) and HCl / dioxane (4N solution, 2.4 mL, 9.61 mmol) was stirred at room temperature for 18 h. The resulting mixture was evaporated under reduced pressure, to give a brown solid which was taken up in water (3 mL), alkalinized with 10% aq. Na_2CO_3 (15 mL), and extracted with a mixture MeOH / $CHCl_3$ 1:9 (4 × 10 mL). The combined organic extracts were dried over anhydrous Na_2SO_4 and concentrated *in vacuo*, to give a light brown oily residue (213 mg), which

was subjected to column chromatography purification (35−70 μm silica gel, CH_2Cl_2 / MeOH / 50% aq. NH_4OH mixtures, gradient elution). On elution with CH_2Cl_2 / MeOH / 50% aq. NH_4OH 98.5:1.5:0.4 to 95:5:0.4, amine **18a** (91 mg, 19% overall yield from amine **16**) was isolated as a white solid; R_f 0.22 (CH_2Cl_2 / MeOH / 50% aq. NH_4OH 95:5:1).

A solution of **18a** (50 mg, 0.09 mmol) in CH_2Cl_2 (2 mL) was filtered through a 0.2 μm PTFE filter, treated with a methanolic solution of HCl (3N solution, 0.3 mL), and evaporated at reduced pressure. The solid was washed with pentane (3 × 2 mL), to give, after drying at 65 ºC / 2 Torr for 48 h, the analytical sample of **18a**·2HCl (49 mg), as a white solid: ^{1}H NMR (400 MHz, CD_3OD) δ 1.80–1.96 (m, 8H, 2'-H_2, 3'-H_2, 6"-H_A, 10"-H_A, 12"-H_A, 13"-H_A), 2.06–2.26 (m, 8H, 3-H_2, 6"-H_B, 8"-H_2, 10"-H_B, 12"-H_B, 13"-H_B), 2.58 (t, J = 6.4 Hz, 2H, 2-H_2), 2.69 (t, J = 5.6 Hz, 2H, 1'-H_2), 2.94 (t, J = 6.0 Hz, 2H, 4'-H_2), 3.32 (m, 1H, 11"-H), 3.38 (m, 1H, 5"-H), 4.07 (t, J = 6.8 Hz, 2H, 4-H_2), 4.85 (s, $^+$NH, NH), 7.10 (d, J = 8.4 Hz, 1H, 4"-H), 7.27 (dd, J = 8.4 Hz, J' = 2.4 Hz, 1H, 3"-H), 7.36 (d, J = 2.4 Hz, 1H, 1"-H), 7.52 (dd, J = 9.2 Hz, J' = 2.4 Hz, 1H, 7'-H), 7.76 (d, J = 2.4 Hz, 1H, 5'-H), 8.46 (d, J = 9.2 Hz, 1H, 8'-H); ^{13}C NMR (100.6 MHz, CD_3OD) δ 21.7 (CH_2, C3'), 22.8 (CH_2, C2'), 24.8 (CH_2, C1'), 26.5 (CH_2, C3), 29.3 (CH_2, C4'), 35.1 (CH_2, C2), 38.6 (CH_2), 38.8 (CH_2) (C6", C12"), 39.5 (CH, d, $J_{C\text{-}F}$ = 13.5 Hz, C5"), 40.4 (CH, d, $J_{C\text{-}F}$ = 12.9 Hz, C11"), 40.7(CH_2, d, $J_{C\text{-}F}$ = 19.4 Hz, C10", C13"), 45.9 (CH_2, d, $J_{C\text{-}F}$ = 20.7 Hz, C8"), 49.1 (CH_2, C4), 58.1 (C, d, $J_{C\text{-}F}$ = 10.3 Hz, C7"), 94.0 (C, d, $J_{C\text{-}F}$ = 179.3 Hz, C9"), 113.4 (C, C9a'), 115.4 (C, C8a'), 119.0 (CH, C5'), 119.6 (CH, C3"), 120.9 (CH, C1"), 126.7 (CH, C7'), 129.0 (CH, C8'), 130.0 (CH, C4"), 138.9 (C, C2"), 140.0 (C, C6'), 140.5 (C, C10a'), 141.0 (C, C4a"), 145.8 (C, C11a"), 151.9 (C, C4a'), 157.9 (C, C9'), 173.5 (C, C1); HRMS (ESI), calcd for [$C_{32}H_{36}{}^{35}ClFN_4O$ + H^+] 547.2634, found 547.2632.

*4.1.12. N-(7-Amino-9-fluoro-7H-5,6,8,9,10,11-hexahydro-5,9:7,11-dimethanobenzo[9]annulen-2-yl)-5-[(6-chloro-1,2,3,4-tetrahydroacridin-9-yl)amino]pentanamide (**18b**)*

This compound was prepared as described for **17a**. From nitrile **11b** (1.10 g, 3.51 mmol), crude carboxylic acid (5.80 g) was obtained as the hydrochloride salt and used in the following step without further purification. From this crude carboxylic acid and amine **16** (575 mg, 1.66 mmol), a brown sticky solid residue (9.84 g) was obtained and subjected to column chromatography purification (35−70 μm silica gel, hexane / EtOAc

/ Et_3N mixtures, gradient elution). On elution with hexane / EtOAc / Et_3N 10:90:0.2 to 0:100:0.2, impure *N*-{7-[(tert-butoxycarbonyl)amino]-9-fluoro-7*H*-5,6,8,9,10,11-hexahydro-5,9:7,11-dimethanobenzo[9]annulen-2-yl}-5-[(6-chloro-1,2,3,4-tetrahydroacridin-9-yl)amino]pentanamide (**17b**, 312 mg) was isolated as a brown oil and used in the following step without further purification; R_f 0.72 (CH_2Cl_2 / MeOH / 50% aq. NH_4OH 95:5:1); LRMS (ESI), 661.3323 (M + H^+).

From *N*-Boc-protected amide **17b** (303 mg) and HCl / dioxane (4N solution, 3.3 mL, 13.0 mmol), a light brown oily residue (261 mg) was obtained and subjected to column chromatography purification (35−70 μm silica gel, CH_2Cl_2 / MeOH / 50% aq. NH_4OH mixtures, gradient elution). On elution with CH_2Cl_2 / MeOH / 50% aq. NH_4OH 98:2:0.4, amine **18b** (94 mg, 10% overall yield from amine **16**) was isolated as a white solid; R_f 0.45 (CH_2Cl_2 / MeOH / 50% aq. NH_4OH 95:5:1).

A solution of **18b** (19 mg, 0.03 mmol) in CH_2Cl_2 (1 mL) was filtered through a 0.2 μm PTFE filter, treated with a methanolic solution of HCl (3N solution, 0.03 mL), and evaporated at reduced pressure. The solid was washed with pentane (3 × 2 mL), to give, after drying at 65 ºC / 2 Torr for 48 h, the analytical sample of **18b**·2HCl (22 mg), as a yellow solid: ^{1}H NMR (400 MHz, CD_3OD) δ 1.78–2.00 (m, 12H, 3-H_2, 4-H_2, 2'-H_2, 3'-H_2, 6"-H_A, 10"-H_A, 12"-H_A, 13"-H_A), 2.06–2.19 (m, 6H, 6"-H_B, 8"-H_2, 10"-H_B, 12"-H_B, 13"-H_B), 2.45 (t, J = 7.2 Hz, 2H, 2-H_2), 2.70 (t, J = 5.2 Hz, 2H, 1'-H_2), 2.99 (t, J = 5.2 Hz, 2H, 4'-H_2), 3.29–3.34 (m, 1H, 11"-H), 3.38 (m, 1H, 5"-H), 3.99 (t, J = 6.8 Hz, 2H, 5-H_2), 4.85 (s, $^+$NH, NH), 7.10 (d, J = 8.4 Hz, 1H, 4"-H), 7.29 (dd, J = 8.4 Hz, J' = 2.0 Hz, 1H, 3"-H), 7.38 (d, J = 2.0 Hz, 1H, 1"-H), 7.53 (dd, J = 9.2 Hz, J' = 2.0 Hz, 1H, 7'-H), 7.76 (d, J = 2.0 Hz, 1H, 5'-H), 8.40 (d, J = 9.2 Hz, 1H, 8'-H); ^{13}C NMR (100.6 MHz, CD_3OD) δ 21.8 (CH_2, C3'), 22.9 (CH_2, C2'), 23.5 (CH_2, C3), 24.8 (CH_2, C1'), 29.4 (CH_2, C4'), 30.7 (CH_2, C4), 36.9 (CH_2, C2), 38.6 (CH_2), 38.8 (CH_2) (C6", C12"), 39.5 (CH, d, $J_{C\text{-}F}$ = 13.0 Hz, C5"), 40.4 (CH, d, $J_{C\text{-}F}$ = 13.1 Hz, C11"), 40.7 (CH_2, d, $J_{C\text{-}F}$ = 19.9 Hz, C10", C13"), 45.9 (CH_2, d, $J_{C\text{-}F}$ = 20.6 Hz, C8"), 49.3 (CH_2, C5), 58.1 (C, d, $J_{C\text{-}F}$ = 10.7 Hz, C7"), 94.0 (C, d, $J_{C\text{-}F}$ = 180.2 Hz, C9"), 113.5 (C, C9a'), 115.5 (C, C8a'), 119.1 (CH, C5'), 119.7 (CH, C3"), 121.0 (CH, C1"), 126.8 (CH, C7'), 128.8 (CH, C8'), 129.9 (CH, C4"), 138.9 (C, C2"), 140.0 (C, C6'), 140.5 (C, C10a'), 141.0 (C, C4a"), 145.7 (C, C11a"), 152.1 (C, C4a'), 157.9 (C, C9'), 174.0 (C, C1); HRMS (ESI), calcd for [$C_{33}H_{38}{}^{35}ClFN_4O$ + H^+] 561.2791, found 561.2796.

4.2. Biological assays

4.2.1. Evaluation of hAChE and hBChE inhibitory activities

The inhibitory activity of the target compounds towards human recombinant AChE and human serum BChE (Sigma, Milan, Italy) was evaluated spectrophotometrically following the method of Ellman *et al*. [61]. The enzyme stock solutions were prepared by dissolving human recombinant AChE or human serum BChE lyophilized powders in 0.1% Triton X-100/0.1 M potassium phosphate, pH 8.0, or in 0.1% aq. gelatin, respectively. The stock solutions of the target compounds (1 mM) were prepared in MeOH. The assay solution consisted of 340 μM 5,5'-dithiobis(2-nitrobenzoic acid) (DTNB), 0.02 unit/mL hAChE or hBChE, and 550 μM acetylthiocholine iodide or butyrylthiocholine iodide, for AChE and BChE, respectively, in 0.1 M potassium phosphate, pH 8.0. Assay solutions with and without the target compounds were preincubated at 37 °C for 20 min, before the addition of the substrate (acetylthiocholine iodide or butyrylthiocholine iodide). Blank solutions containing all components except the enzymes were prepared in parallel to correct for non-enzymatic hydrolysis of the substrates. Initial rate assays were performed at 37 °C with a Jasco V-530 double beam spectrophotometer. At least five increasing concentrations of the target compounds, which led to 20–80% inhibition of the enzymatic activities, were assayed. IC_{50} values were calculated using Microcal Origin 3.5 software (Microcal Software, Inc).

4.2.2. Evaluation of NMDA receptor antagonist activity

The functional assay for the determination of the antagonistic activity of the target compounds at the NMDA receptors was performed using primary cultures of rat cerebellar granule neurons, which were prepared following established protocols [49]. Cells were grown on 10 mm poly-L-lysine coated glass cover slips and used for the experiments after 6–9 days *in vitro*. Cells were loaded with 6 μM Fura-2 AM (ThermoFisher-Invitrogen) for 30 min, and then, the coverslip was mounted on a quartz cuvette containing a Mg^{2+}-free Locke-Hepes (LH) buffer using a special holder. Measurements were performed using a Perkin Elmer LS-55 fluorescence spectrometer equipped with a fast-filter accessory, under mild agitation at 37 ºC. Analysis from each sample was recorded real-time during 1400 s. After stimulation with NMDA (100 μM, in the presence of 10 μM glycine), increasing cumulative concentrations of the target compounds were added (range: 0.1–100 μM). To avoid precipitation, the tested compounds were dissolved in LH buffer containing a final concentration of 1.8% β-cyclodextrin. The percentages of inhibition at every tested concentration were analyzed

using a non-linear regression curve fitting (variable slope) by using the software GraphPad Prism 5.0.

4.2.3. Evaluation of BACE-1 inhibitory activity

The inhibitory activity of the target compounds towards human recombinant BACE-1 (β-secretase, Invitrogen) was evaluated by employing the Panvera peptide as substrate [71]. Ten μL of substrate (250 nM final concentration) were added to 10 μL of solution of the target compounds or buffer in control wells (20 mM sodium acetate, pH 4.5, containing CHAPS 0.1% w/v). To start the reaction 10 μL of BACE-1 enzyme were added (12.91 mU). The enzyme was left to react for 1 h at 37 ºC. The fluorescence signal was read at λem = 544 nm (λex = 590 nm) after adding 10 μL of STOP solution (2.5M NaOAc). The DMSO concentration in the final mixture was maintained below 5% (v/v) to guarantee no significant loss of enzyme activity. The fluorescence intensities with and without inhibitor were compared and the percent of inhibition due to the presence of the target compounds was calculated. The background signal was measured in control wells containing all the reagents, except BACE-1, and was subtracted. The % of inhibition due to the presence of test compounds was calculated by the following expression: $100 – (IF_i/IF_o \times 100)$, where IF_i and IF_o are the fluorescence intensities obtained for BACE-1 in the presence and in the absence of inhibitor, respectively.

4.2.4. Evaluation of Aβ42 and tau anti-aggregating activities

The inhibitory activities of the target compounds towards Aβ42 and tau aggregation were assessed using intact *E. coli* cells, as previously described [51,65,66]. *E. coli* BL21 (DE3) competent cells were transformed with the pET28a vector (Novagen, Inc., Madison, WI, USA), which carryies the DNA sequence of Aβ42, or with pTARA, which contains the RNA-polymerase gen of T7 phage (T7RP) under the control of the promoter PBAD, and were then transformed with the pRKT42 vector, encoding four repeats of tau protein in two inserts. Ten mL of M9 minimal medium containing 50 μg/mL of kanamycin (for Aβ42 overexpression) or 0.5% of glucose, 50 μg/mL of ampicillin and 12.5 μg/mL of chloramphenicol (for tau overexpression) were inoculated with a colony of BL21 (DE3) cells bearing the plasmids. The volume of overnight culture necessary to get a 1:500 dilution was added into fresh M9 minimal medium

containing 50 μg/mL of kanamycin and 250 μM of Th-S (for Aβ42 overexpression) or 0.5% of glucose, 50 μg/mL of ampicillin, 12.5 μg/mL of chloramphenicol, and 250 μM of Th-S (for tau overexpression). The cultures were grown overnight at 37 ºC and 250 rpm until cell density reached OD_{600} = 0.6. A volume of 980 μL of the cultures was transferred into 1.5 mL eppendorf tubes that contained 10 μL of a solution of the target compound in DMSO and 10 μL of isopropyl 1-thio-β-D-galactopyranoside (IPTG) at 100 mM (for Aβ42 overexpression) or 10 μL of arabinose at 25% (for tau overexpression), thereby leading to a final inhibitor concentration of 10 μM. The resulting cultures were grown overnight at 37 °C and 1400 rpm with a Thermomixer (Eppendorf, Hamburg, Germany). The same amount of DMSO without the target compound was added to the sample as a negative control (maximal amount of Aβ42 or tau), whereas non-induced samples (in the absence of IPTG or arabinose) were prepared as positive controls (absence of Aβ42 or tau), and to assess the potential intrinsic toxicity of the target compounds.

The effects of the target compounds on Aβ42 or tau aggregation were assessed using a previously described fluorescence assay [51,65,66], by employing a 2500 mM stock solution of thioflavin-S (Th-S, T1892, Sigma, St. Louis, MO, USA) in double-distilled water (Milli-Q system, Millipore, USA), and measuring the Th-S spectra on an Aminco Bowman Series 2 luminescence spectrophotometer (Aminco-Bowman AB2, SLM Aminco, Rochester, NY, USA) in the range 460–600 nm at 25 °C, with an excitation wavelength of 440 nm and slit widths of 4 nm, and an emission wavelength of 485 nM.

4.2.5. Evaluation of brain permeability: PAMPA-BBB assay

The brain permeability (P_e) of the target compounds was determined by the *in vitro* parallel artificial membrane permeability assay for blood-brain barrier penetration of Di *et al*. [70], which employs a lipid extract of porcine brain membrane in PBS/EtOH 70:30. The assay was validated by comparison of the experimental and reported P_e values of a set of fourteen commercial drugs (Table 2), and the following correlation was obtained: P_e (exp) = 1.5758 P_e (lit) – 1.1459 (R^2 = 0.9241). From this equation and the limits established by Di *et al.* for BBB permeation, the threshold for high BBB permeation (CNS+) was set at *Pe* (10^{-6} cm/s) > 5.16; whereas the range for low BBB permeation (CNS–) was set at *Pe* (10^{-6} cm/s) < 2.01, and that for uncertain BBB permeation (CNS±) at 5.16 > *Pe* (10^{-6} cm/s) > 2.01.

Table 2

Experimental and reported BBB permeability values (*Pe* 10^{-6} cm/s) of the commercial drugs used for assay validation.

Drug	Reported *Pe*[a]	Experimental *Pe*[b]
Cimetidine	0.0	0.7 ± 0.1
Lomefloxacin	1.1	0.8 ± 0.1
Norfloxazin	0.1	0.9 ± 0.1
Ofloxazin	0.8	1.0 ± 0.1
Hydrocortisone	1.9	1.4 ± 0.1
Piroxicam	2.5	2.1 ± 0.1
Clonidine	5.3	6.5 ± 0.1
Corticosterone	5.1	6.7 ± 0.1
Imipramine	13.0	12.3 ± 0.1
Promazine	8.8	13.8 ± 0.3
Progesterone	9.3	16.8 ± 0.3
Desipramine	12.0	17.8 ± 0.1
Testosterone	17.0	26.4 ± 0.3
Verapamil	16.0	28.6 ± 0.3

[a] Taken from [70]. [b] Values are expressed as the mean ± SD of three independent experiments.

Conflicts of interest

There are no conflicts to declare.

Acknowledgments

This work was supported by Ministerio de Ciencia, Innovación y Universidades, Agencia Estatal de Investigación (AEI) and FEDER (SAF2017-82771-R) and Generalitat de Catalunya (GC) (2017SGR106). Fellowships from GC to F.J.P.-A., from Ministerio de Educación, Cultura y Deporte to C.P. and A.L.T., and from Lifelong Learning Programme / Erasmus to D.P., and a contract from the Juan de la Cierva program of Ministerio de Economía y Competitividad to A.E. (grant JCI-2012-12193) are gratefully acknowledged.

Appendix A. Supplementary material

Supplementary data to this article can be found online at http://dx.doi.org/. These data include copies of the ^{1}H and ^{13}C NMR spectra of the tested compounds.

References

[1] M. Prince, A. Wimo, M. Guerchet, G.-C. Ali, Y.-T. Wu, M. Prina, World Alzheimer Report 2015. The global impact of dementia. An analysis of prevalence, incidence, cost & trends; Alzheimer's Disease International: London, 2015; http://www.alz.co.uk.

[2] S.H. Kim, N. Kandiah, J.-L. Hsu, C. Suthisisang, C. Udommongkol, A. Dash, Beyond symptomatic effects: potential of donepezil as a neuroprotective agent and disease modifier in Alzheimer's disease, Br. J. Pharmacol. 174 (2017) 4224–4232.

[3] D. Muñoz-Torrero, Acetylcholinesterase inhibitors as disease-modifying therapies for Alzheimer's disease, Curr. Med. Chem. 15 (2008) 2433–2445.

[4] L.A. Mohamed, H. Qosa, A. Kaddoumi, Age-related decline in brain and hepatic clearance of amyloid-beta is rectified by the cholinesterase inhibitors donepezil and rivastigmine in rats, ACS Chem. Neurosci. 6 (2015) 725–736.

[5] J. Folch, O. Busquets, M. Ettcheto, E. Sánchez-López, R.D. Castro-Torres, E. Verdaguer, M.L. Garcia, J. Olloquequi, G. Casadesús, C. Beas-Zarate, C. Pelegri, J. Vilaplana, C. Auladell, A. Camins, Memantine for the treatment of dementia: A review on its current and future applications, J. Alzheimers Dis. 62 (2018) 1223–1240.

[6] K. Takahashi-Ito, M. Makino, K. Okado, T. Tomita, Memantine inhibits β-amyloid aggregation and disassembles preformed β-amyloid aggregates, Biochem. Biophys. Res. Commun. 493 (2017) 158–163.

[7] S.A. Lipton, Paradigm shift in neuroprotection by NMDA receptor blockade: memantine and beyond, Nat. Rev. Drug Discovery 5 (2006) 160–170.

[8] J.L. Cummings, T. Morstof, K. Zhong, Alzheimer's disease drug-development pipeline: few candidates, frequent failures, Alzheimers Res. Ther. 6 (2014) 37.

[9] S.O. Bachurin, E.V. Bovina, A.A. Ustyugov, Drugs in clinical trials for Alzheimer's disease: The major trends, Med. Res. Rev. 37 (2017) 1186–1225.

[10] C.-X. Gong, F. Liu, K. Iqbal, Multifactorial hypothesis and multi-targets for Alzheimer's disease, J. Alzheimers Dis. 64 (2018) S107–S117.

[11] A. Cavalli, M.L. Bolognesi, A. Minarini, M. Rosini, V. Tumiatti, M. Recanatini, C. Melchiorre, Multi-target-directed ligands to combat neurodegenerative diseases, J. Med. Chem. 51 (2008) 347–372.

[12] R. Morphy, Z. Rankovic, Designing multiple ligands – medicinal chemistry strategies and challenges, Curr. Pharm. Des. 15 (2009) 587–600.

[13] E. Proschak, H. Stark, D. Merk, Polypharmacology by design: A medicinal chemist's perspective on multitargeting compounds, J. Med. Chem. 62 (2019), 420–444.

[14] M.L. Bolognesi, Polypharmacology in a single drug: Multitarget drugs, Curr. Med. Chem. 20 (2013) 1639–1645.

[15] Y. Yabuki, K. Matsuo, K. Hirano, Y. Shinoda, S. Moriguchi, K. Fukunaga, Combined memantine and donepezil treatment improves behavioral and psychological symptoms of dementia-like behaviors in olfactory bulbectomized mice, Pharmacology 99 (2017) 160–171.

[16] A. Atri, S.B. Hendrix, V. Pejovi, R.K. Hofbauer, J. Edwards, J.L. Molinuevo, S.M. Graham, Cumulative, additive benefits of memantine-donepezil combination over component monotherapies in moderate to severe Alzheimer's dementia: a pooled area under the curve analysis, Alzheimers Res. Ther. 7 (2015) 28.

[17] P.T. Francis, C.G. Parsons, R.W. Jones, Rationale for combining glutamatergic and cholinergic approaches in the symptomatic treatment of Alzheimer's disease, Expert. Rev. Neurother. 12 (2012) 1351–1365.

[18] R.T. Owen, Memantine and donepezil: a fixed drug combination for the treatment of moderate to severe Alzheimer's dementia, Drugs Today 52 (2016) 239–248.

[19] S.L. Greig, Memantine ER/donepezil: a review in Alzheimer's disease, CNS Drugs 29 (2015) 963–970.

[20] M.G. Savelieff, G. Nam, J. Kang, H.J. Lee, M. Lee, M.H. Lim, Development of multifunctional molecules as potential therapeutic candidates for Alzheimer's disease, Parkinson's disease, and amyotrophic lateral sclerosis in the last decade, Chem. Rev. 119 (2019) 1221–1322.

[21] M. de Freitas Silva, K.S.T. Dias, V.S. Gontijo, C.J.C. Ortiz, C. Viegas, Multi-target directed drugs as a modern approach for drug design towards Alzheimer's disease: an update, Curr. Med. Chem. 25 (2018) 3491–3525.

[22] D. Muñoz-Torrero, Multitarget anti-Alzheimer hybrid compounds: Do they work in vivo?, in Design of Hybrid Molecules for Drug Development, M. Decker (Ed.), 2017, Elsevier, Amsterdam, pp.167–192.

[23] Y. Duarte, A. Fonseca, M. Gutiérrez, F. Adasme-Carreño, C. Muñoz-Gutierrez, J. Alzate-Morales, L. Santana, E. Uriarte, R. Álvarez, M.J. Matos, Novel coumarin-quinoline hybrids: Design of multitarget compounds for Alzheimer's disease, ChemistrySelect 4 (2019) 551–558.

[24] J. Hu, T. Pan, B. An, Z. Li, X. Li, L. Huang, Synthesis and evaluation of clioquinol-rolipram/roflumilast hybrids as multitarget-directed ligands for the treatment of Alzheimer's disease, Eur. J. Med. Chem. 163 (2019) 512–526.

[25] L. Pisani, R.M. Iacobazzi, M. Catto, M. Rullo, R. Farina, N. Denora, S. Cellamare, C.D. Altomare, Investigating alkyl nitrates as nitric oxide releasing precursors of multitarget acetylcholinesterase-monoamine oxidase B inhibitors, Eur. J. Med. Chem. 161 (2019) 292–309.

[26] Z. Wang, J. Hu, X. Yang, X. Feng, X. Li, L. Huang, A.S.C. Chan, Design, synthesis, and evaluation of orally bioavailable quinoline-indole derivatives as innovative multitarget-directed ligands: Promotion of cell proliferation in the adult murine hippocampus for the treatment of Alzheimer's disease, J. Med. Chem. 61 (2018) 1871–1894.

[27] Ó. M. Bautista-Aguilera, J. Budni, F. Mina, E. B. Medeiros, W. Deuther-Conrad, J. M. Entrena, I. Moraleda, I. Iriepa, F. López-Muñoz, J. Marco-Contelles, Contilisant, a tetratarget small molecule for Alzheimer's disease therapy combining cholinesterase, monoamine oxidase inhibition and H3R antagonism with sigma 1R agonism profile, J. Med. Chem 61 (2018) 6937–6943.

[28] A. Gandini, M. Bartolini, D. Tedesco, L. Martinez-Gonzalez, C. Roca, N. E. Campillo, J. Zaldivar-Diez, C. Perez, G. Zuccheri, G. Miti, A. Feoli, S. Castellano, S. Petralla, B. Monti, M. Rossi, F. Moda, G. Legname, A. Martinez, M. L. Bolognesi, Tau-centric multitarget approach for Alzheimer's disease: Development of first-in-class dual glycogen synthase kinase 3*β* and tau aggregation inhibitors, J. Med. Chem. 61 (2018) 7640–7656.

[29] J. Lalut, G. Santoni, D. Karila, C. Lecoutey, A. Davis, F. Nachon, I. Silman, J. Sussman, M. Weik, T. Maurice, P. Dallemagne, C. Rochais, Novel multitarget-directed ligands targeting acetylcholinesterase and σ1 receptors as lead compounds for treatment of Alzheimer's disease: Synthesis, evaluation, and structural characterization of their complexes with acetylcholinesterase, Eur. J. Med. Chem. 162 (2019) 234–248.

[30] G. Cheng, P. Xu, M. Zhang, J. Chen, R. Sheng, Y. Ma, Resveratrol-maltol hybrids as multi-target-directed agents for Alzheimer's disease, Bioorg. Med. Chem. 26 (2018) 5759–5765.

[31] P. Cai, S.-Q. Fang, H.-L. Yang, X.-L. Yang, Q.-H. Liu, L.-Y. Kong, X.-B. Wang, Donepezil-butylated hydroxytoluene (BHT) hybrids as Anti-Alzheimer's disease agents with cholinergic, antioxidant, and neuroprotective properties, Eur. J. Med. Chem. 157 (2018) 161–176.

[32] M. Chioua, E. Buzzi, I. Moraleda, I. Iriepa, M. Maj, A. Wnorowski, C. Giovannini, A. Tramarin, F. Portali, L. Ismaili, P. López-Alvarado, M.L. Bolognesi, K. Jóźwiak, J.C. Menéndez, J. Marco-Contelles, M. Bartolini, Tacripyrimidines, the first tacrine-dihydropyrimidine hybrids, as multi-target-directed ligands for Alzheimer's disease, Eur. J. Med. Chem. 155 (2018) 839–846.

[33] A. Hiremathad, R.S. Keri, A.R. Esteves, S.M. Cardoso, S. Chaves, M.A. Santos, Novel tacrine-hydroxyphenylbenzimidazole hybrids as potential multitarget drug candidates for Alzheimer's disease, Eur. J. Med. Chem. 148 (2018) 255–267.

[34] X.-Y. Jiang, T.-K. Chen, J.-T. Zhou, S.-Y. He, H.-Y. Yang, Y. Chen, W. Qu, F. Feng, H.-P. Sun, Dual GSK-3β/AChE inhibitors as a new strategy for multitargeting anti-Alzheimer's disease drug discovery, ACS Med. Chem. Lett. 9 (2018) 171–176.

[35] A. Więckowska, T. Wichur, J. Godyń, A. Bucki, M. Marcinkowska, A. Siwek, K. Więckowski, P. Zaręba, D. Knez, M. Głuch-Lutwin, G. Kazek, G. Latacz, K. Mika, M. Kołaczkowski, J. Korabecny, O. Soukup, M. Benkova, K. Kieć-Kononowicz, S. Gobec, B. Malawska, Novel multitarget-directed ligands aiming at symptoms and causes of Alzheimer's disease, ACS Chem. Neurosci. 9 (2018) 1195–1214.

[36] D. Dolles, M. Hoffmann, S. Gunesch, O. Marinelli, J. Möller, G. Santoni, A. Chatonnet, M.J. Lohse, H.-J. Wittmann, A. Strasser, M. Nabissi, T. Maurice, M. Decker, Structure–activity relationships and computational investigations into the development of potent and balanced dual-acting butyrylcholinesterase inhibitors and human cannabinoid receptor 2 ligands with pro-cognitive in vivo profiles, J. Med. Chem. 61 (2018) 1646–1663.

[37] N. Chufarova, K. Czarnecka, R. Skibiński, M. Cuchra, I. Majsterek, P. Szymański, New tacrine-acridine hybrids as promising multifunctional drugs for potential treatment of Alzheimer's disease, Arch. Phar. 351 (2018) 1800050.

[38] M. Rosini, E. Simoni, M. Bartolini, A. Cavalli, L. Ceccarini, N. Pascu, D.W. McClymont, A. Tarozzi, M.L. Bolognesi, A. Minarini, V. Tumiatti, V. Andrisano, I.R. Mellor, C. Melchiorre, Inhibition of acetylcholinesterase, β-amyloid aggregation, and NMDA receptors in Alzheimer's disease: A promising direction for the multi-target-directed ligands gold rush, J. Med. Chem. 51 (2008) 4381–4384.

[39] S.O. Bachurin, E.F. Shevtsova, G.F. Makhaeva, V.V. Grigoriev, N.P. Boltneva, N.V. Kovaleva, S.V. Lushchekina, P.N. Shevtsov, M.E. Neganova, O.M. Redkozubova, E.V. Bovina, A.V. Gabrelyan, V.P. Fisenko, V.B. Sokolov, A.Y. Aksinenko, V. Echeverria, G.E. Barreto, G. Aliev, Novel conjugates of aminoadamantanes with carbazole derivatives as potential multitarget agents for AD treatment, Sci. Rep. 7 (2017) 45627.

[40] Y. Rook, K.-U. Schnmidtke, F. Gaube, D. Shepmann, B. Wünsch, J. Heilmann, J. Lehmann, T. Winckler, Bivalent β-carbolines as potential multitarget anti-Alzheimer agents, J. Med. Chem. 53 (2010) 3611–3617.

[41] O. Soukup, D. Jun, J. Zdarova-Karasova, J. Patocka, K. Musilek, J. Korabecny, J. Krusek, M. Kaniakova, V. Sepsova, J. Mandikova, F. Trejtnar, M. Pohanka, L. Drtinova, M. Pavlik, G. Tobin, K. Kuca, A resurrection of 7-MEOTA: a comparison with tacrine, Curr. Alzheimer Res. 10 (2013) 893–906.

[42] E. Simoni, S. Daniele, G. Bottegoni, D. Pizzirani, M.L. Trincavelli, L. Goldoni, G. Tarozzo, A. Reggiani, C. Martini, D. Piomelli, C. Melchiorre, M. Rosini, A. Cavalli, Combining galantamine and memantine in multitargeted, new chemical entities potentially useful in Alzheimer's disease. J. Med. Chem. 55 (2012) 9708–9721.

[43] A.M. Reggiani, E. Simoni, R. Caporaso, J. Meunier, E. Keller, T. Maurice, A. Minarini, M. Rosini, A. Cavalli, *In vivo* characterization of ARN14140, a memantine/galantamine-based multi-target compound for Alzheimer's disease. Sci. Rep. 6 (2016) 33172.

[44] Z. Gazova, O. Soukup, V. Sepsova, K. Siposova, L. Drtinova, P. Jost, K. Spilovska, J. Korabecny, E. Nepovimova, D. Fedunova, M. Horak, M. Kaniakova, Z.-J. Wang, A.K. Hamouda, K. Kuca, Multi-target-directed therapeutic potential of 7-methoxytacrine-adamantylamine heterodimers in the Alzheimer's disease treatment, Biochim. Biophys. Acta 1863 (2017) 607–619.

[45] K. Spilovska, J. Korabecny, J. Kral, A. Horova, K. Musilek, O. Soukup, L. Drtinova, Z. Gazova, K. Siposova, K. Kuca, 7-Methoxytacrine-adamantylamine heterodimers as cholinesterase inhibitors in Alzheimer's disease treatment – Synthesis, biological evaluation and molecular modeling studies, Molecules 18 (2013) 2397–2418.

[46] M.D. Duque, P. Camps, L. Profire, S. Montaner, S. Vázquez, F.X. Sureda, J. Mallol, M. López-Querol, L. Naesens, E. De Clercq, S.R. Prathalingam, J.M. Kelly, Synthesis and pharmacological evaluation of (2-oxaadamant-1-yl)amines, Bioorg. Med. Chem. 17 (2009) 3198–3206.

[47] P. Camps, M.D. Duque, S. Vázquez, L. Naesens, E. De Clercq, F.X. Sureda, M. López-Querol, A. Camins, M. Pallàs, S.R. Prathalingam, J.M. Kelly, V. Romero, D. Ivorra, D. Cortés, Synthesis and pharmacological evaluation of several ring-contracted amantadine analogs, Bioorg. Med. Chem. 16 (2008) 9925–9936.

[48] M.D. Duque, P. Camps, E. Torres, E. Valverde, F.X. Sureda, M. López-Querol, A. Camins, S.R. Prathalingam, J.M. Kelly, S. Vázquez, New oxapolycyclic cage amines with NMDA receptor antagonist and trypanocidal activities, Bioorg. Med. Chem. 18 (2010) 46–57.

[49] E. Torres, M.D. Duque, M. López-Querol, M.C. Taylor, L. Naesens, C. Ma, L.H. Pinto, F.X. Sureda, J.M. Kelly, S. Vázquez, Synthesis of benzopolycyclic

cage amines: NMDA receptor antagonist, trypanocidal and antiviral activities, Bioorg. Med. Chem. 20 (2012) 942–948.

[50] E. Valverde, F.X. Sureda, S. Vázquez, Novel benzopolycyclic amines with NMDA receptor antagonist activity, Bioorg. Med. Chem. 22 (2014) 2678–2683.

[51] I. Sola, E. Aso, D. Frattini, I. López-González, A. Espargaró, R. Sabaté, O. Di Pietro, F. J. Luque, M. V. Clos, I. Ferrer, D. Muñoz-Torrero, Novel levetiracetam derivatives that are effective against the Alzheimer-like phenotype in mice: synthesis, in vitro, ex vivo and in vivo efficacy studies, J. Med. Chem. 58 (2015) 6018–6032.

[52] O. Di Pietro, F.J. Pérez-Areales, J. Juárez-Jiménez, A. Espargaró, M.V. Clos, B. Pérez, R. Lavilla, R. Sabaté, F.J. Luque, D. Muñoz-Torrero, Tetrahydrobenzo[*h*][1,6]naphthyridine-6-chlorotacrine hybrids as a new family of anti-Alzheimer agents targeting β-amyloid, tau, and cholinesterase pathologies, Eur. J. Med. Chem. 84 (2014) 107–117.

[53] E. Viayna, I. Sola, M. Bartolini, A. De Simone, C. Tapia-Rojas, F. G. Serrano, R. Sabaté, J. Juárez-Jiménez, B. Pérez, F. J. Luque, V. Andrisano, M. V. Clos, N. C. Inestrosa, D. Muñoz-Torrero, Synthesis and multi-target biological profiling of a novel family of rhein derivatives as disease-modifying anti-Alzheimer agents, J. Med. Chem. 57 (2014) 2549–2567.

[54] F.J. Pérez-Areales, O. Di Pietro, A. Espargaró, A. Vallverdú-Queralt, C. Galdeano, I.M. Ragusa, E. Viayna, C. Guillou, M.V. Clos, B. Pérez, R. Sabaté, R.M. Lamuela-Raventós, F.J. Luque, D. Muñoz-Torrero, Shogaol-huprine hybrids: Dual antioxidant and anticholinesterase agents with β-amyloid and tau anti-aggregating properties, Bioorg. Med. Chem. 22 (2014) 5298–5307.

[55] V.E. Gregor, M.R. Emmerling, C. Lee, C. J. Moore. The synthesis and *in vitro* acetylcholinesterase and butyrylcholinesterase inhibitory activity of tacrine (Cognex ®) derivatives, Bioorg. Med. Chem. Lett. 2 (1992) 861–864.

[56] C.G. Parsons, G. Quack, I. Bresink, L. Baran, E. Przegalinski, W. Kostowski, P. Krzascik, S. Hartmann, W. Danysz, Comparison of the potency, kinetics and voltage-dependency of a series of uncompetitive NMDA receptor antagonists *in vitro* with anticonvulsive and motor impairment activity *in vivo*, Neuropharmacology 34 (1995) 1239–1258.

[57] M.-K. Hu, C.-F. Lu, A facile synthesis of bis-tacrine isosteres, Tetrahedron Lett. 41 (2000) 1815–1818.

[58] P. Camps, X. Formosa, C. Galdeano, T. Gómez, D. Muñoz-Torrero, M. Scarpellini, E. Viayna, A. Badia, M.V. Clos, A. Camins, M. Pallàs, M. Bartolini, F. Mancini, V. Andrisano, J. Estelrich, M. Lizondo, A. Bidon-Chanal, F.J. Luque, Novel donepezil-based inhibitors of acetyl- and butyrylcholinesterase and acetylcholinesterase-induced *β*-amyloid aggregation, J. Med. Chem. 51 (2008) 3588–3598.

[59] M. Barniol-Xicota, A. Escandell, E. Valverde, E. Julián, E. Torrents, S. Vázquez, Antibacterial activity of novel benzopolycyclic amines, Bioorg. Med. Chem. 23 (2015) 290–296.

[60] R.M. Lane, S.G. Potkin, A. Enz, Targeting acetylcholinesterase and butyrylcholinesterase in dementia, Int. J. Neuropsychopharmacol. 9 (2006) 101–124.

[61] G.L. Ellman, K.D. Courtney, V. Andres, R.M. Featherstone, A new and rapid colorimetric determination of acetylcholinesterase activity, Biochem. Pharmacol. 7 (1961) 88–95.

[62] K. Takahashi-Ito, M. Makino, K. Okado, T. Tomita, Memantine inhibits β-amyloid aggregation and disassembles preformed β-amyloid aggregates, Biochem. Biophys. Res. Commun. 493 (2017) 158–163.

[63] C. Galdeano, E. Viayna, I. Sola, X. Formosa, P. Camps, A. Badia, M.V. Clos, J. Relat, M. Ratia, M. Bartolini, F. Mancini, V. Andrisano, M. Salmona, C. Minguillón, G.C. González-Muñoz, M.I. Rodríguez-Franco, A. Bidon-Chanal, F.J. Luque, D. Muñoz-Torrero, Huprine–tacrine heterodimers as anti-amyloidogenic compounds of potential interest against Alzheimer's and prion diseases, J. Med. Chem. 55 (2012) 661–669.

[64] F.J. Pérez-Areales, N. Betari, A. Viayna, C. Pont, A. Espargaró, M. Bartolini, A. De Simone, J.F. Rinaldi Alvarenga, B. Pérez, R. Sabate, R.M. Lamuela-Raventós, V. Andrisano, F.J. Luque, D. Muñoz-Torrero, Design, synthesis and multitarget biological profiling of second-generation anti-Alzheimer rhein–huprine hybrids, Fut. Med. Chem. 9 (2017) 965–981.

[65] S. Pouplana, A. Espargaro, C. Galdeano, E. Viayna, I. Sola, S. Ventura, D. Muñoz-Torrero, R. Sabate, Thioflavin-S staining of bacterial inclusion bodies for the fast, simple, and inexpensive screening of amyloid aggregation inhibitors, Curr. Med. Chem. 21 (2014) 1152–1159.

[66] A. Espargaró, A. Medina, O. Di Pietro, D. Muñoz-Torrero, R. Sabate, Ultra rapid in vivo screening for anti-Alzheimer anti-amyloid drugs, Sci. Rep. 6 (2016) 23349.

[67] A. Espargaró, C. Pont, P. Gamez, D. Muñoz-Torrero, R. Sabate, Amyloid pan-inhibitors: One family of compounds to cope with all conformational diseases, ACS Chem. Neurosci. 10 (2019), 1311–1317.

[68] C.A. Lipinski, F. Lombardo, B.W. Dominy, P.J. Feeney, Experimental and computational approaches to estimate solubility and permeability in drug discovery and development settings, Adv. Drug Delivery Rev. 23 (1997) 3–25.

[69] R. Morphy, Z. Rankovic, Designing multiple ligands – medicinal chemistry strategies and challenges, Curr. Pharm. Des. 15 (2009) 587–600.

[70] L. Di, E.H. Kerns, K. Fan, O.J. McConnell, G.T. Carter, High throughput artificial membrane permeability assay for blood-brain barrier. Eur. J. Med.Chem. 38 (2003) 223–232.

[71] A. Tarozzi, M. Bartolini, L. Piazzi, L. Valgimigli, R. Amorati, C. Bolondi, A. Djemil, F. Mancini, V. Andrisano, A. Rampa, From the dual function lead AP2238 to AP2469, a multi-target-directed ligand for the treatment of Alzheimer's disease, Pharmacol. Res. Perspect. 2 (2014) e00023.